

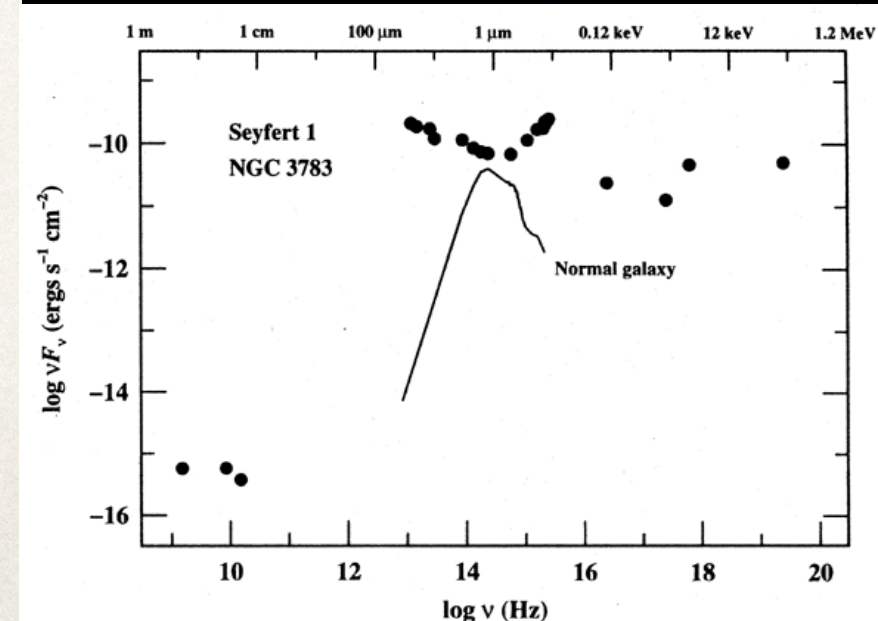
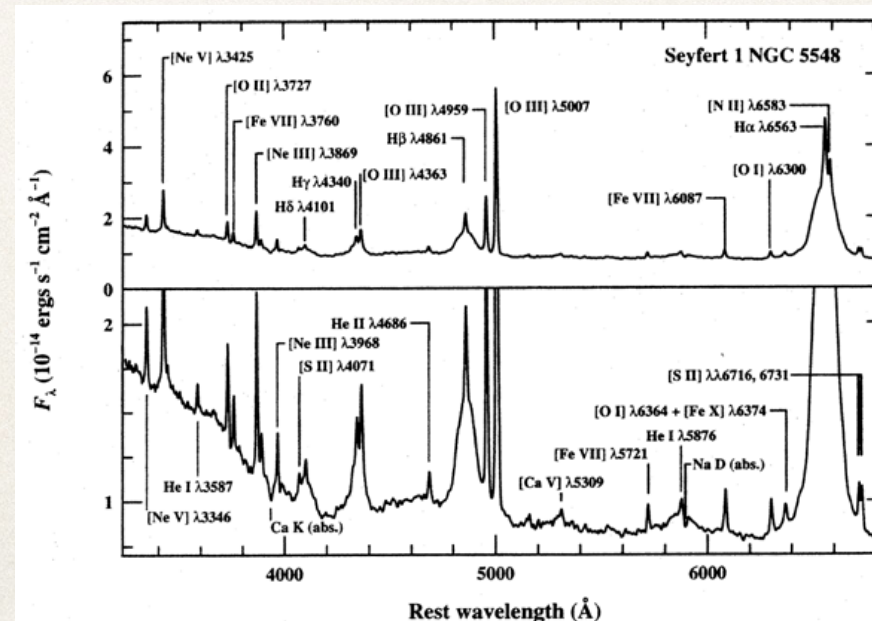
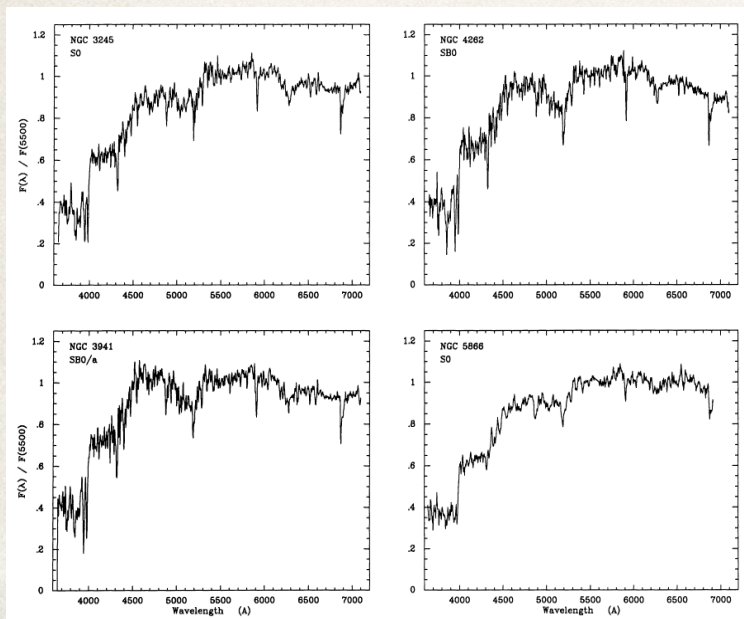
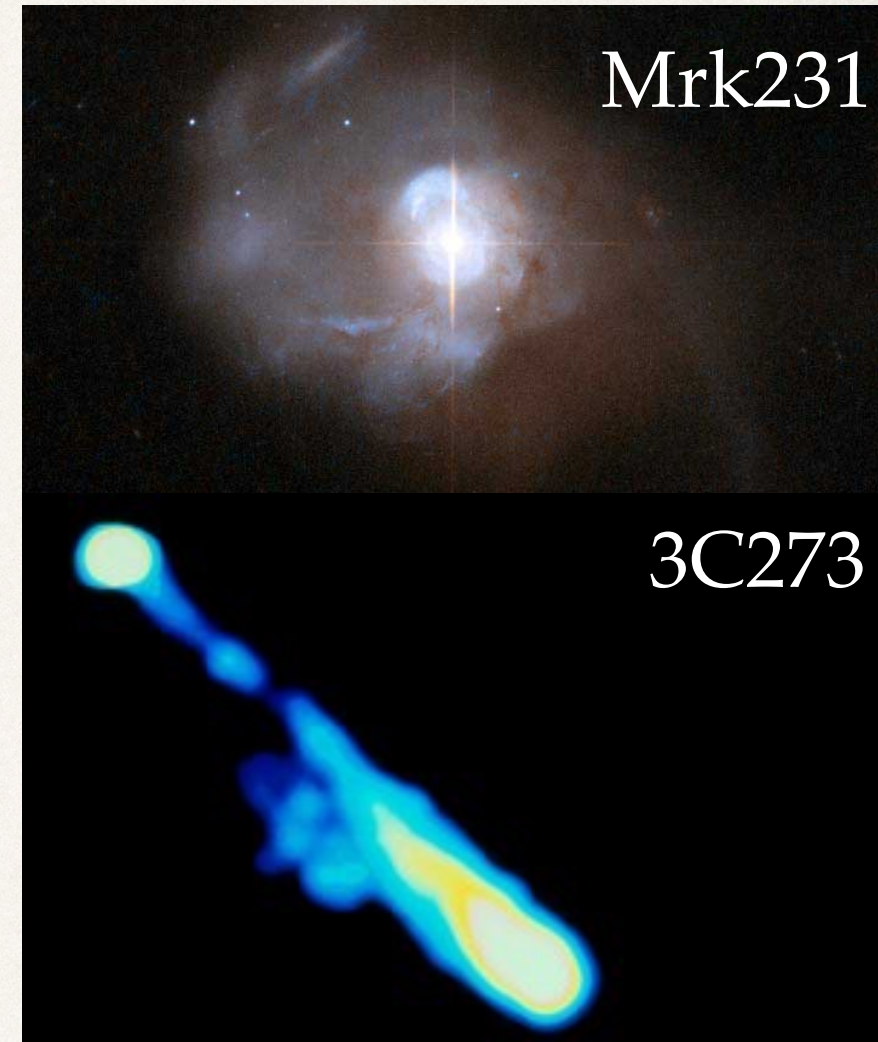
X-rays from AGN Jets

Preeti Kharb

National Centre for Radio Astrophysics - Tata Institute of Fundamental Research

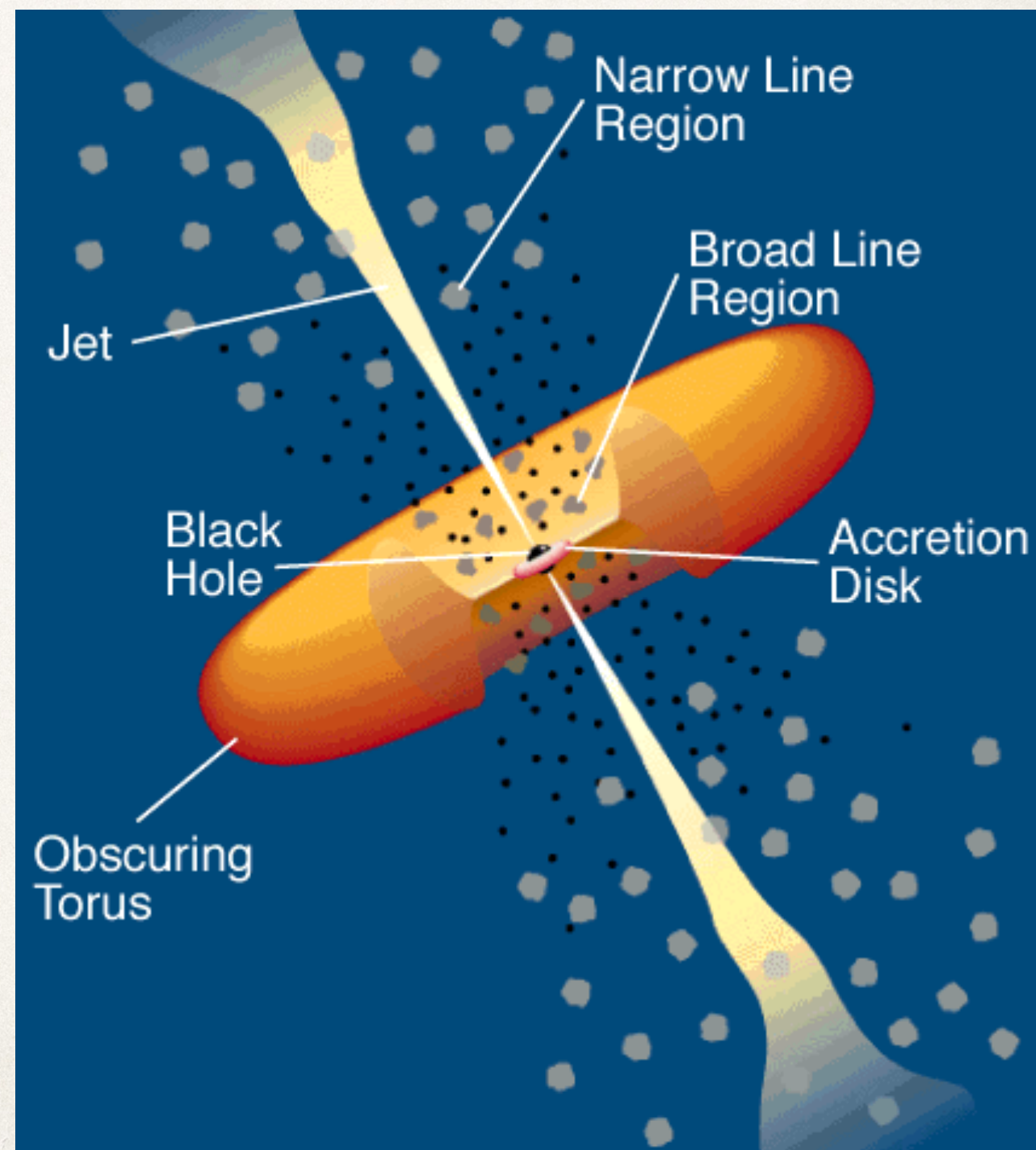
ACTIVE GALACTIC NUCLEI

- ❖ Bright compact regions in galaxy centres ($L_{\text{AGN}} \sim 10^{11} - 10^{14} L_{\odot}$) which can outshine the light from the entire galaxy ($\sim 10^{11}$ stars)
- ❖ C. Seyfert (1943) — Bright star-like nucleus + Peculiar spectrum. **Seyfert galaxies.**
- ❖ M. Schmidt, B. Oke (1963) — Optical counterpart of radio source 3C273 was a galaxy with emission line spectrum at $z=0.158$. **Quasars.**
- ❖ AGN emission is Broad-band and Non-stellar in origin

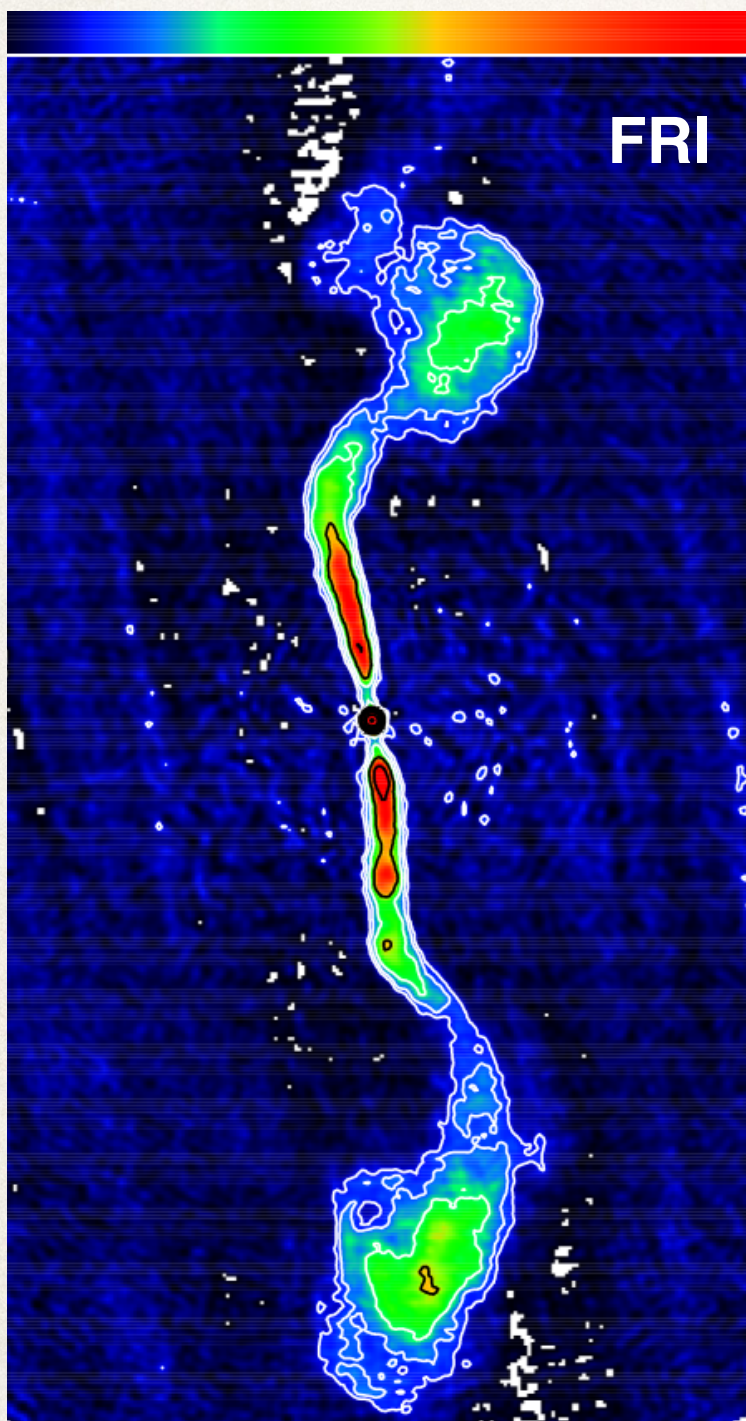


AGN MODEL

- ❖ Supermassive black hole (SMBH) $\sim 10^6 - 10^9 M_{\odot}$
- ❖ Accretion Disk (AD)
- ❖ Broad-line Region (BLR), line widths $\sim 1000 - 10,000 \text{ km/s}$
- ❖ Narrow-line Region (NLR), line widths $\sim 500 \text{ km/s}$
- ❖ Dusty Obscuring Torus
- ❖ Relativistic Jets launched from AD - SMBH interface
- ❖ Power-law spectrum + High degree of Linear polarisation \rightarrow Radio Synchrotron emission
- ❖ *Jet Launching & Acceleration mechanisms, Jet Composition Unclear*



Radio-loud AGN

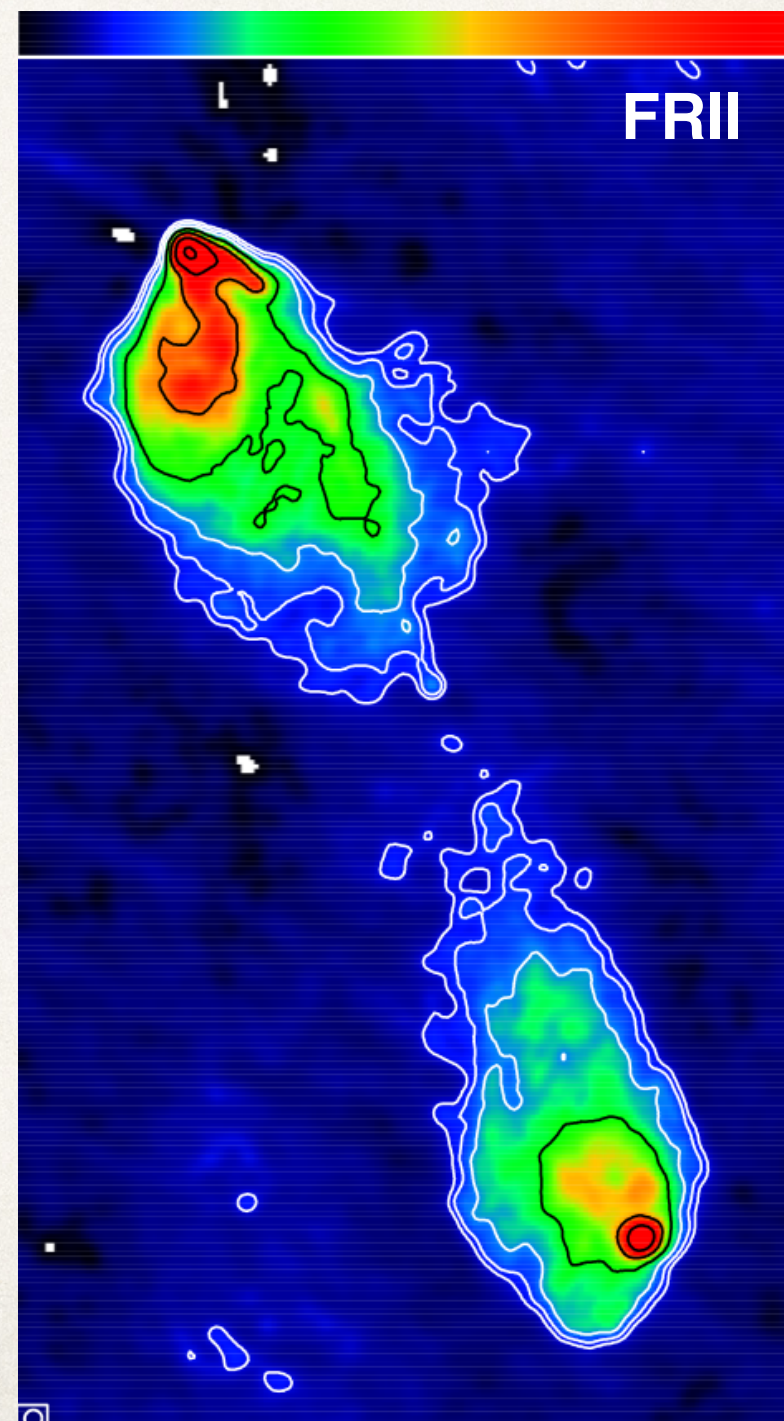


- ❖ Large Radio Jets of extents 10s to 100s of kilo-parsec

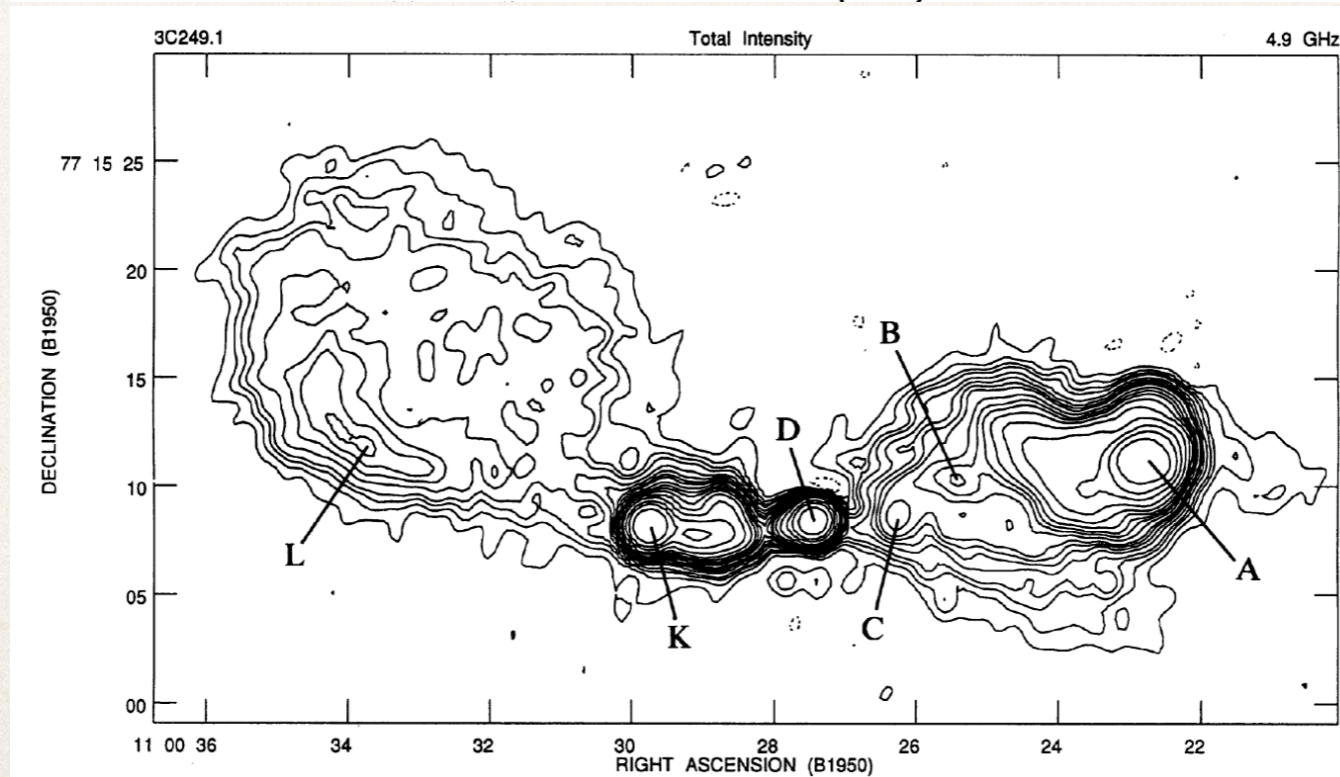
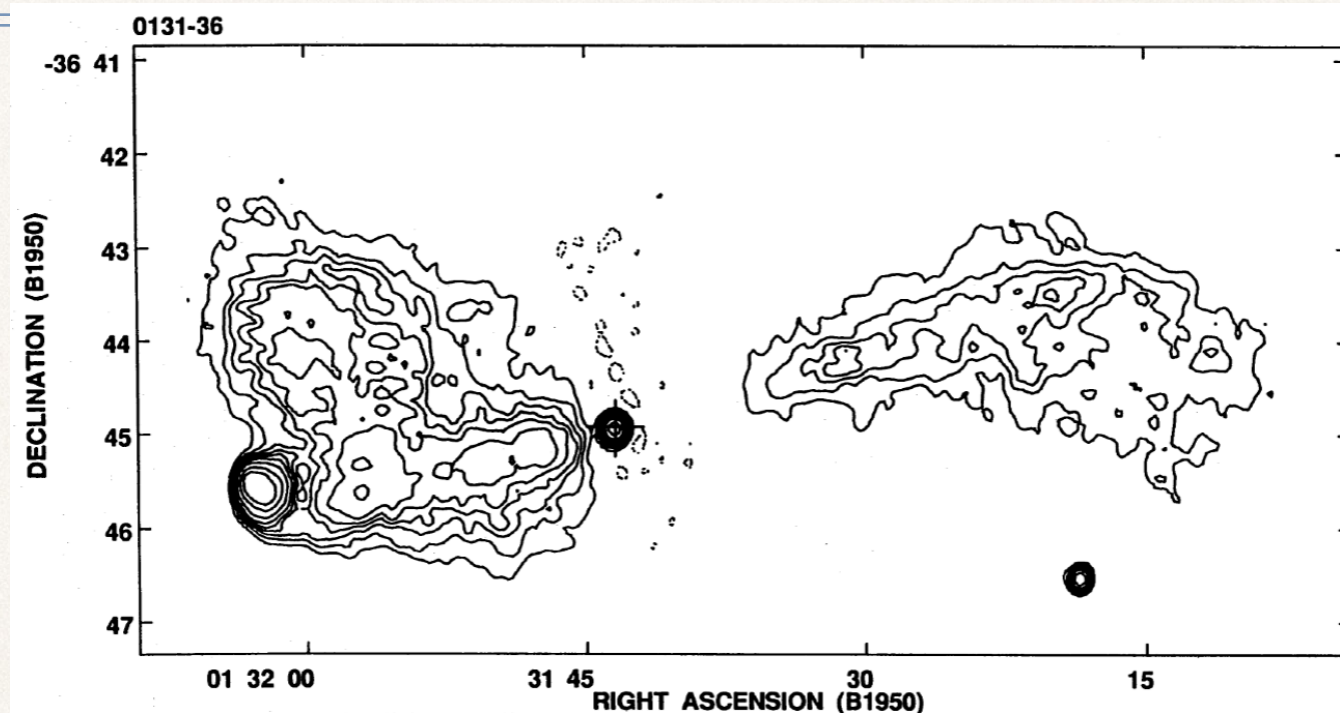
- ❖ Fanaroff-Riley (FR) Dichotomy

- ❖ $L_{178} \approx 2 \times 10^{25} \text{ W / Hz}$

(Fanaroff & Riley, 1974)

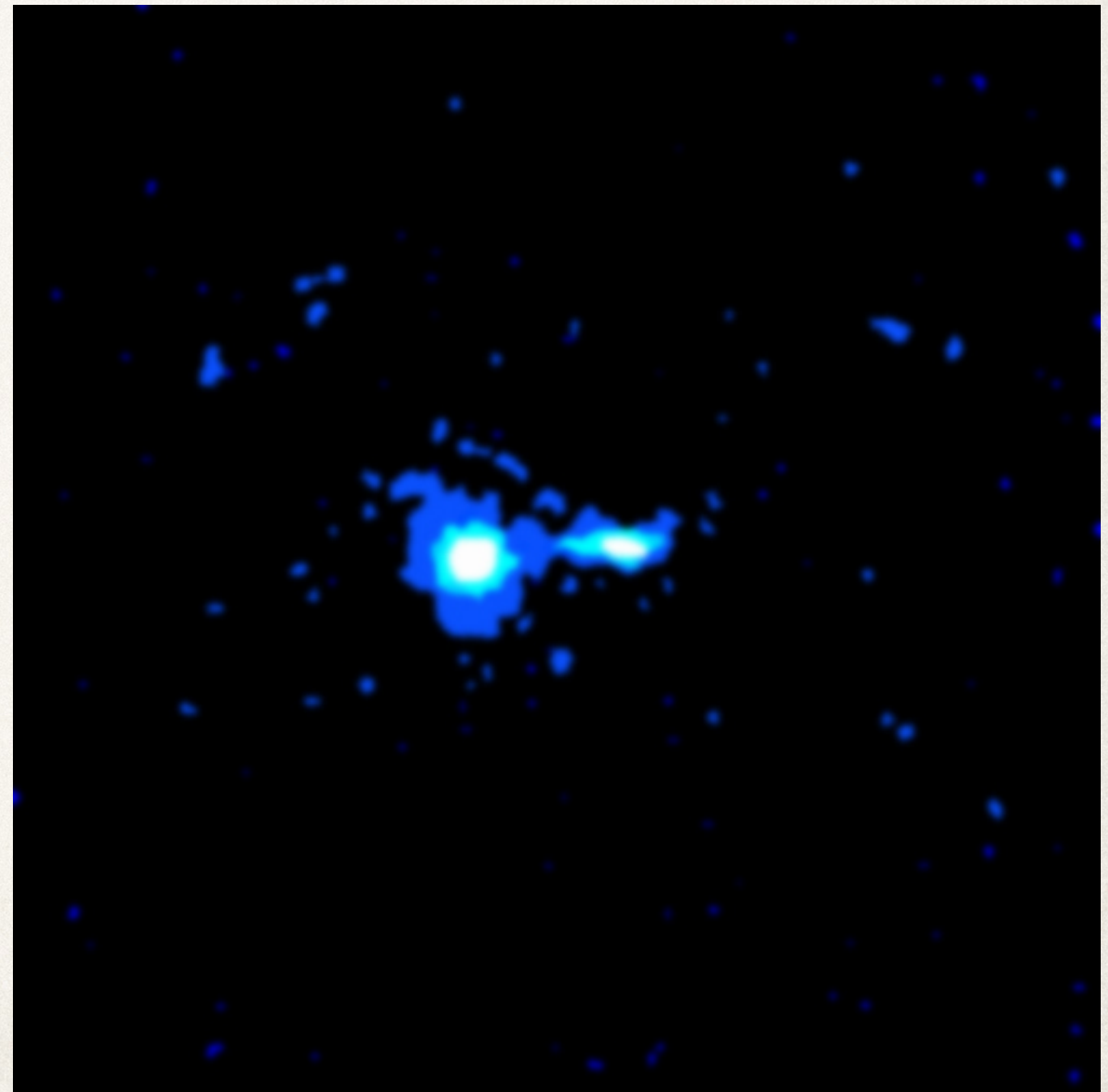


Hybrid / Intermediate Sources

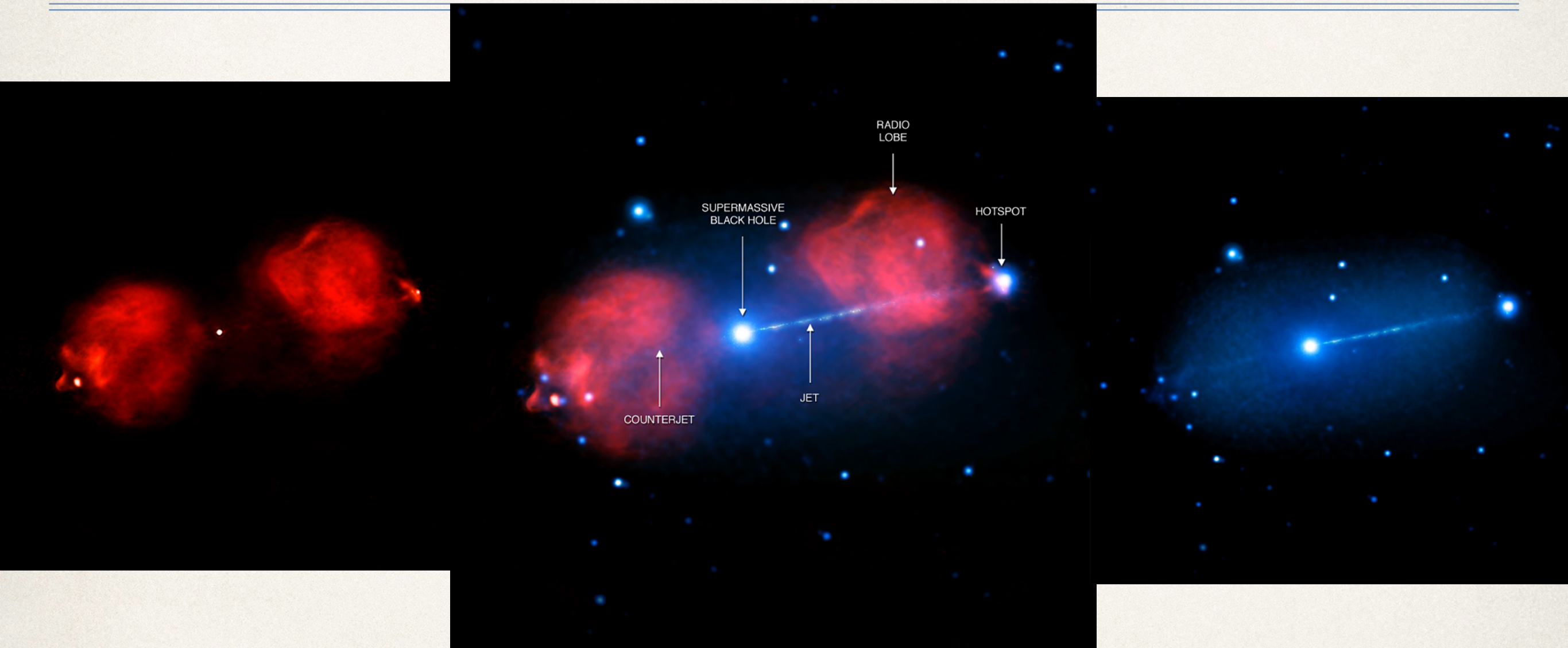


Chandra's First Look: X-ray Jets

- ❖ In August 1999 Chandra ACIS observed its first celestial target PKS 0637-752 during the initial focusing of the telescope
- ❖ High z (0.654) Quasar
- ❖ 100 kpc X-ray Jet (Schwartz+2000)

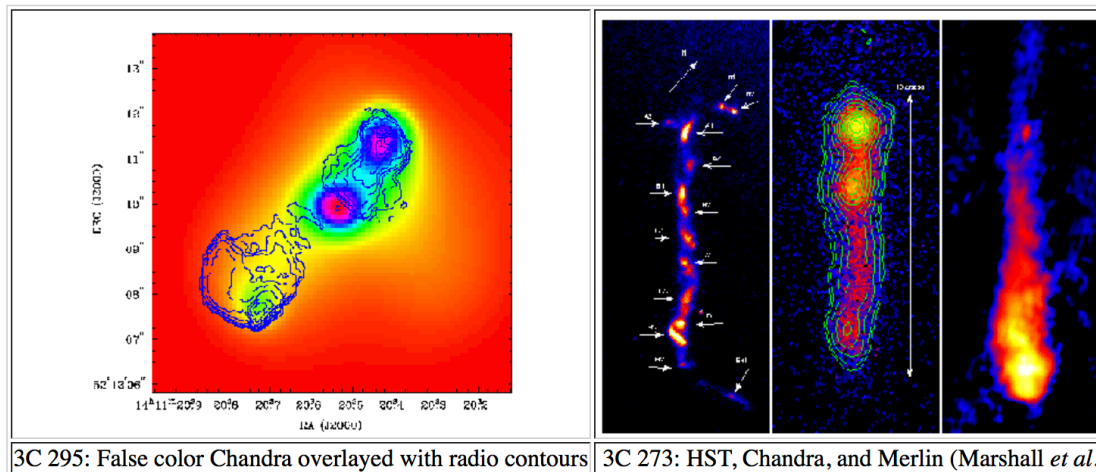


X-rays from AGN Jets



Pictor A

XJET: X-RAY EMISSION FROM EXTRAGALACTIC RADIO JETS



3C 295: False color Chandra overlaid with radio contours

3C 273: HST, Chandra, and Merlin (Marshall *et al.*)

MOTIVATION

This website is meant to serve as a clearing house for radio galaxies and quasars for which X-ray emission has been detected which is associated with radio jets, i.e. knots and hotspots. As resources permit, we will also provide downloadable fits images for public use. If you would like to donate a fits image, have a new example to add to the list, or find erroneous or incomplete information, please email [D. Harris](mailto:D.Harris)

- [Chandra Flux Maps for Downloading](#)
- [Index of FITS images](#)
- [Image Policy](#)
- [Image doc template \(for image submission\).](#)

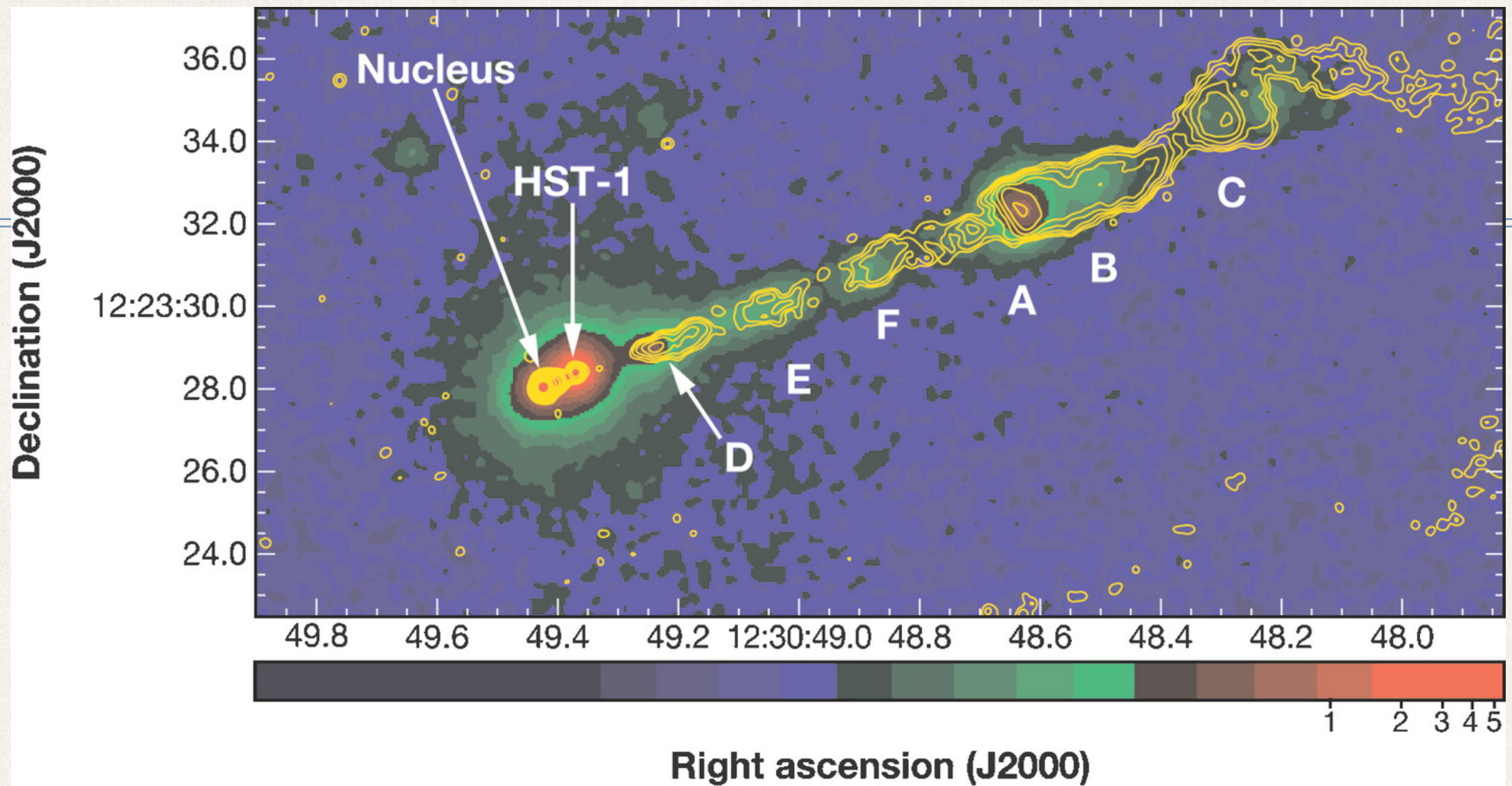
<http://hea-www.harvard.edu/XJET/>
 ~120 X-ray jets

RADIO SOURCES WITH JET RELATED X-RAY EMISSION

Generic Name	R.A. (J2000) hh:mm:ss.s	Dec. (J2000) dd:mm:ss.s	z	Class	X-ray Features	Assoc. optical	Assoc. radio	PA w.r.t core	Dist. (H=71) (Mpc)	kpc/" (H=71)
3C6.1	00:16:31.1	+79:16:49.9	0.8404	FRII RG	both HS	?	yes	N, S	5342	7.6
3C9	00:20:25.2	+15:40:54.7	2.012	LDQ	jet, CL	?	yes	SE, NW	15,850	8.5
3C15	00:37:04.1	-01:09:08.5	0.0730	FRI RG	knot, lobes	yes	yes	-30	326	1.4
3C17	00:38:20.5	-02:07:40.7	0.22	FR2 RG	knot	yes	yes	SE	1081	3.5
NGC315	00:57:48.9	+30:21:08.8	0.0165	FRI RG	inner jet knots	?	same as X-ray	NW	70.6	0.33
3C31	01:07:24.9	+32:25:45.0	0.0167	FRI RG	inner 8" jet	yes	jet	-20	71.4	0.34
0106+013	01:08:38.8	+01:35:0.317	2.099	CDQ	knot	?	same as X-ray	S	16702	8.43
3C33	01:08:52.9	+13:20:13.8	0.0597	FRII RG	both hotspots	yes	yes	20, 200 deg	264	1.14
3C47	01:36:24.4	+20:57:27.4	0.425	LDQ	hsS	no	yes	S	2322	5.5
4C+35.03	02:09:38.6	+35:47:50.9	0.0369	FRI RG	inner jet	no	yes	-46	160	0.72
PKS0208-512	02:10:46.3	-51:01:02.9	0.999	CDQ	jet/knot	no	yes	SW	6626	8.04
3C66B	02:23:11.4	+43:00:31.2	0.0215	FRI RG	inner 8" jet	jet	jet	45	92	0.43
0234+285	02:37:52.4	+28:48:08.9	1.213	CDQ	jet	?	similar as X-ray	N	8445	8.36
0313-192	03:15:52.1	-19:06:44.3	0.067	FRI RG	inner jet	?	same as X-ray	S	298	1.27
3C83.1	03:18:15.7	+41:51:27.9	0.0251	FRI RG	E and W knots	??	similar	E and W	108	0.5
PKS0405-12	04:07:48.4	-12:11:36.6	0.574	CDQ	hs	same as X-ray	yes	N	3338	6.5
3C109	04:13:40.4	+11:12:13.8	0.3056	FRII RG	hsS	no	yes	S	1574	4.5
PKS0413-21	04:16:04.4	-20:56:27.5	0.808	CDQ	jet/knot	no	yes	SE	5087	7.545
3C111	04:18:21.3	+38:01:35.8	0.0491	FRII RG	knots	?	similar as X-ray	NE	215	0.95
3C120	04:33:11.1	+05:21:15.6	0.0330	Sy I	inner jet; 4" knot; 25" knot; 80" knot	some	same as X-ray	NW	143	0.65
3C123	04:37:04.4	+29:40:13.7	0.2177	FRII RG	hsE, hsW	no	same as X-ray	110, W	1068	3.49
3C129	04:49:09.1	+45:00:39.3	0.0208	FRI RG	two inner knots	no	jet	14	89	0.42
0454-463	04:55:50.8	-46:15:58.7	0.858	CDQ	knot	?	similar as X-ray	SE	5481	7.7
PictorA	05:19:49.7	-45:46:44.5	0.0350	FRII RG	linear jet, W hs, CL	W hs	W hs, CL	-80	152	0.69

Page maintained by

Teddy Cheung
Francesco Massaro
Dan Harris



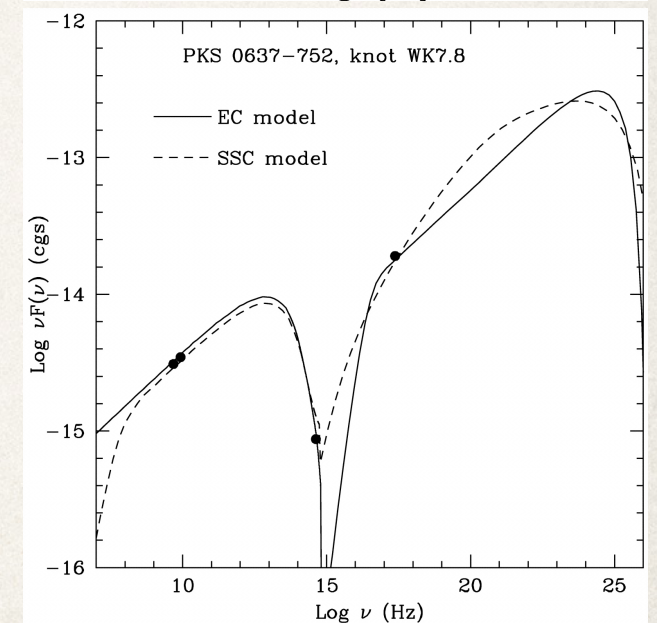
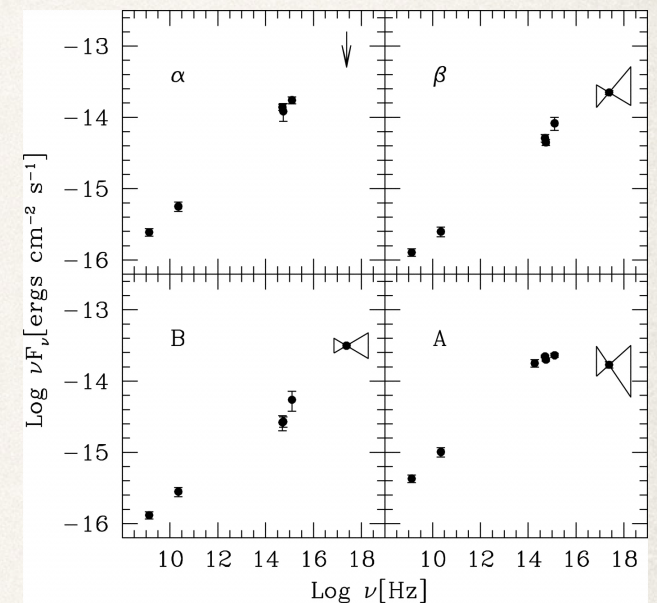
AR Harris DE, Krawczynski H. 2006.
 Annu. Rev. Astron. Astrophys. 44:463–506

M87

X-ray emission mechanism in AGN jets not universally established

X-ray Emission Mechanisms

- ❖ **Thermal Bremsstrahlung:** predicted n_e is $> n_e$ upper limit from Faraday RM values — Ruled out for AGN jets
- ❖ **Synchrotron:** $\gamma > 10^7$ needed + *in situ* acceleration as electron lifetimes are of the order of 10 yrs for Equipartition B-field B_{eq} — works in FRI Jets
- ❖ **Synchrotron-self-Compton:** need B fields far from B_{eq} . Large energy budget — works in some hotspots but not in Jets
- ❖ **IC/CMB:** need highly relativistic kpc-scale jets ($\Gamma \sim 10$) at small angles to line of sight — works in FRII Jets although radio data (indirectly) suggest $\Gamma \sim 2$
- ❖ **IC/CMB:** does not work in some blazar jets with Fermi gamma-ray detection



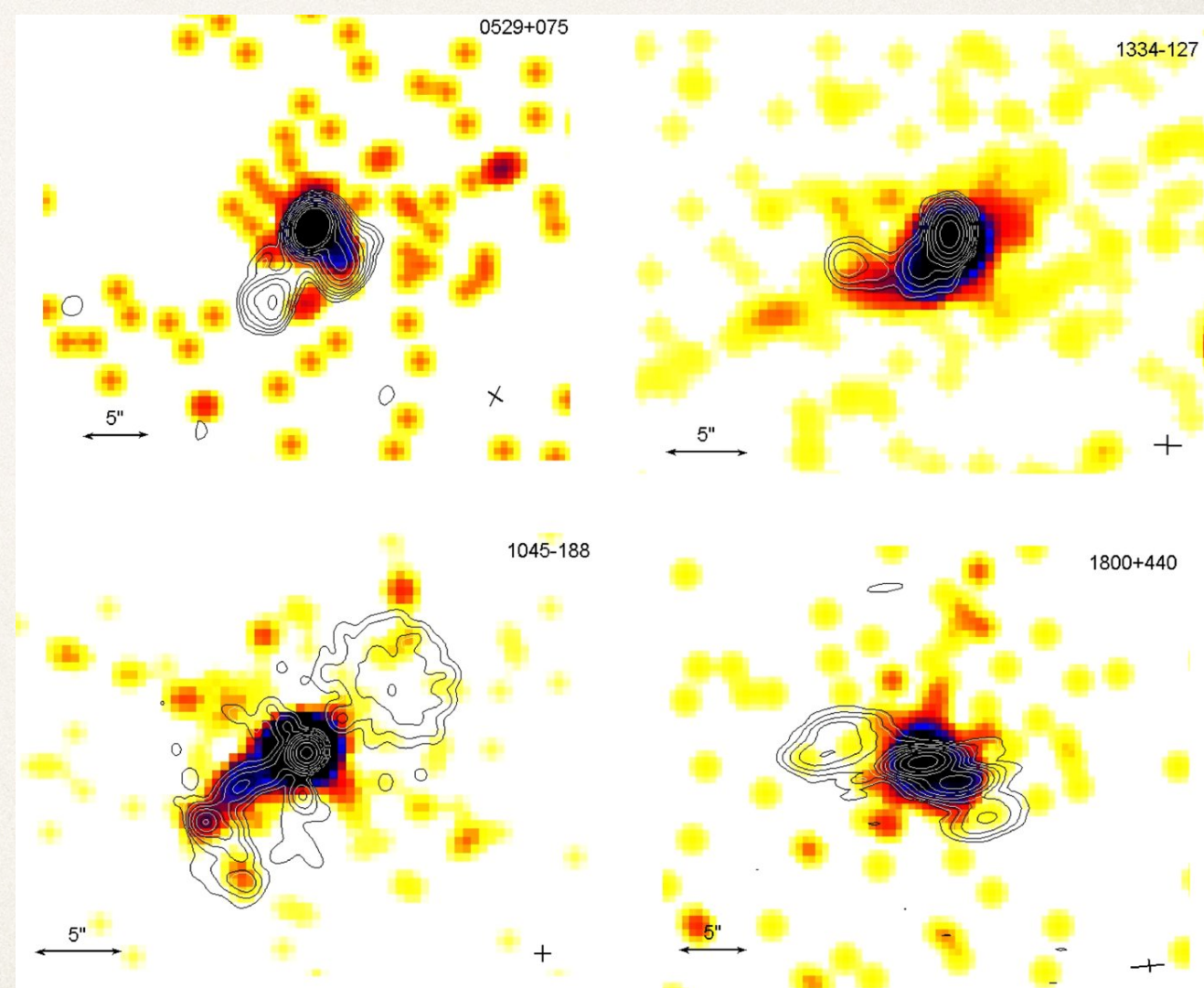
FRI 3C371 Sambruna+ 2007

FRII 0637-752 Tavecchio+ 2000

Snapshot X-ray Observations

- ❖ Complete flux-density-limited **MOJAVE** sample — 135 blazars (Lister & Homan 2005)
- ❖ MOJAVE-Chandra sample (MCS): 27 quasars with (i) $S_{1.4\text{ext}}^{1.4} > 100$ mJy (ii) Radio Extent $> 3''$
- ❖ 10 ks Chandra revealed X-ray jets in $\approx 80\%$ of MCS quasars
- ❖ As MCS quasars lie at $z = 0.5 - 1$ (3 sources at $z > 1$) high detection rate consistent with IC/CMB, as CMB photon energy density increases with z as $(1+z)^4$

Hogan, Lister, Kharb, Marshall, Cooper, 2011

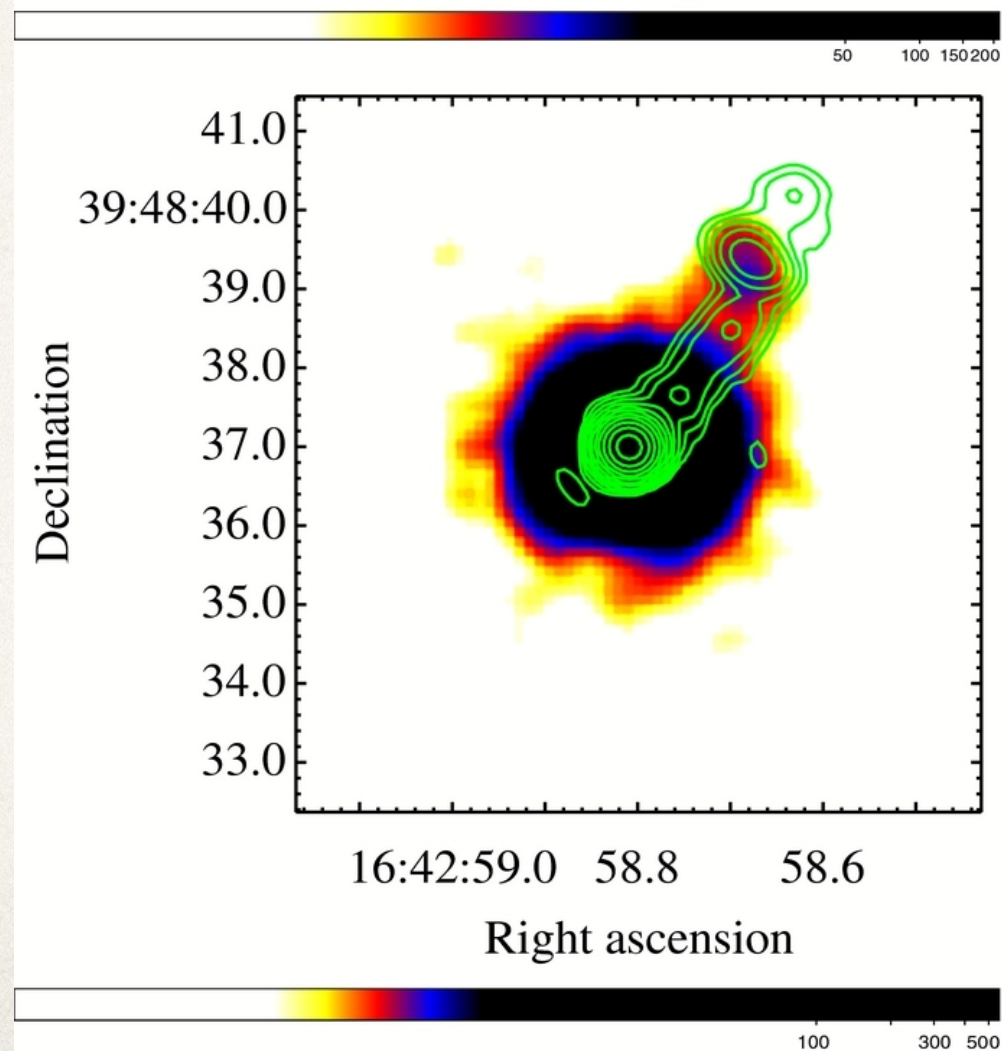
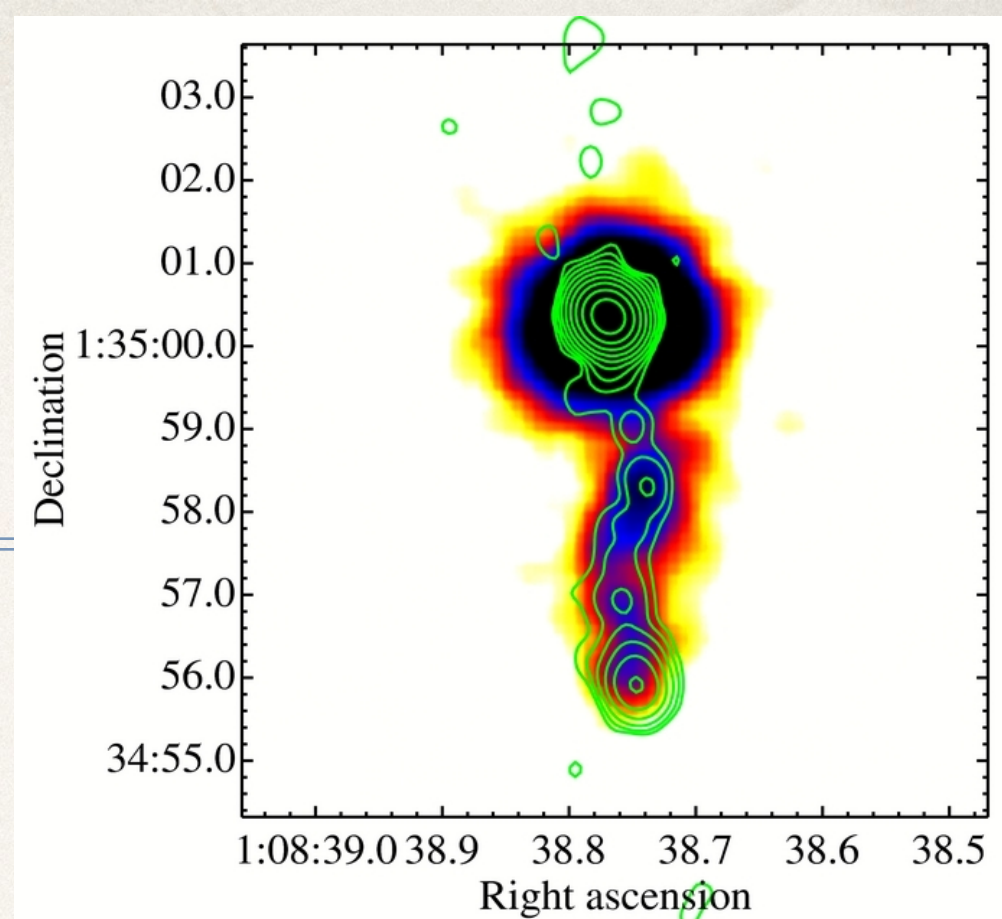


Monitoring Of Jets in AGN with VLBA Experiments

Chandra-HST Observations

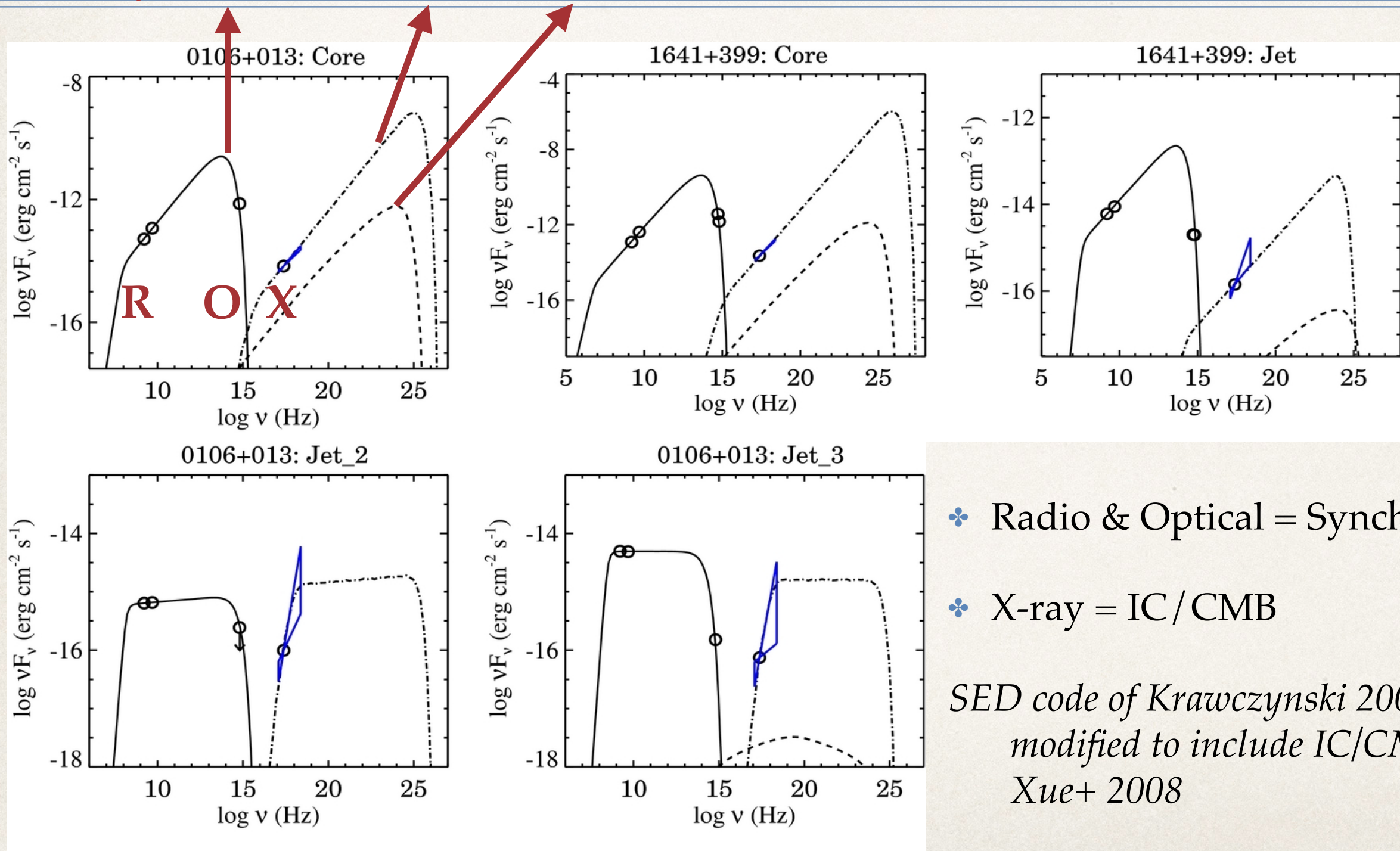
- ❖ Members of MCS with X-ray jets detected
- ❖ Chandra ACIS-S and HST ACS/F475W
- ❖ Excellent spatial correlation with the radio emission: wiggles & bends
- ❖ Optical emission only from the jet termination regions: 2 knots in 0106+013, hotspot/jet bend in 3C 345

Kharb, Lister, Marshall, Hogan, 2012



Spectral Energy Distribution (SED)

Synchrotron IC/CMB SSC

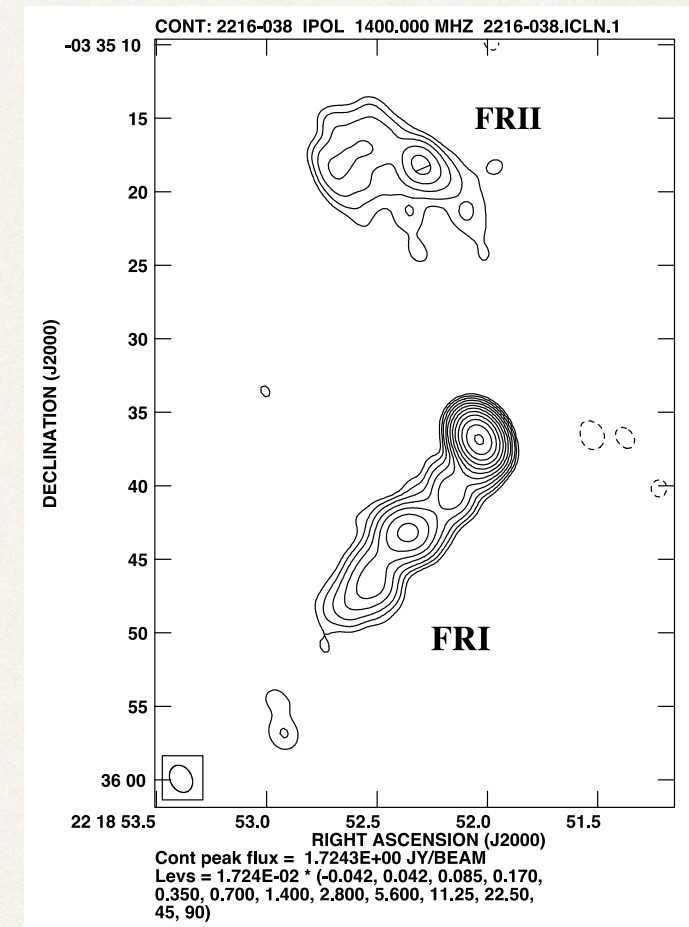
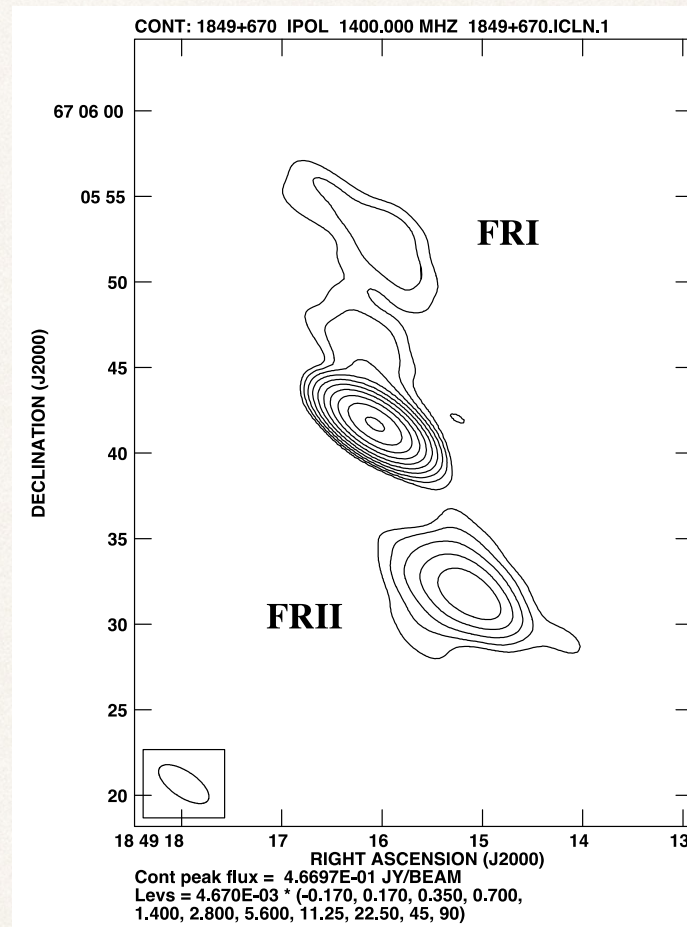
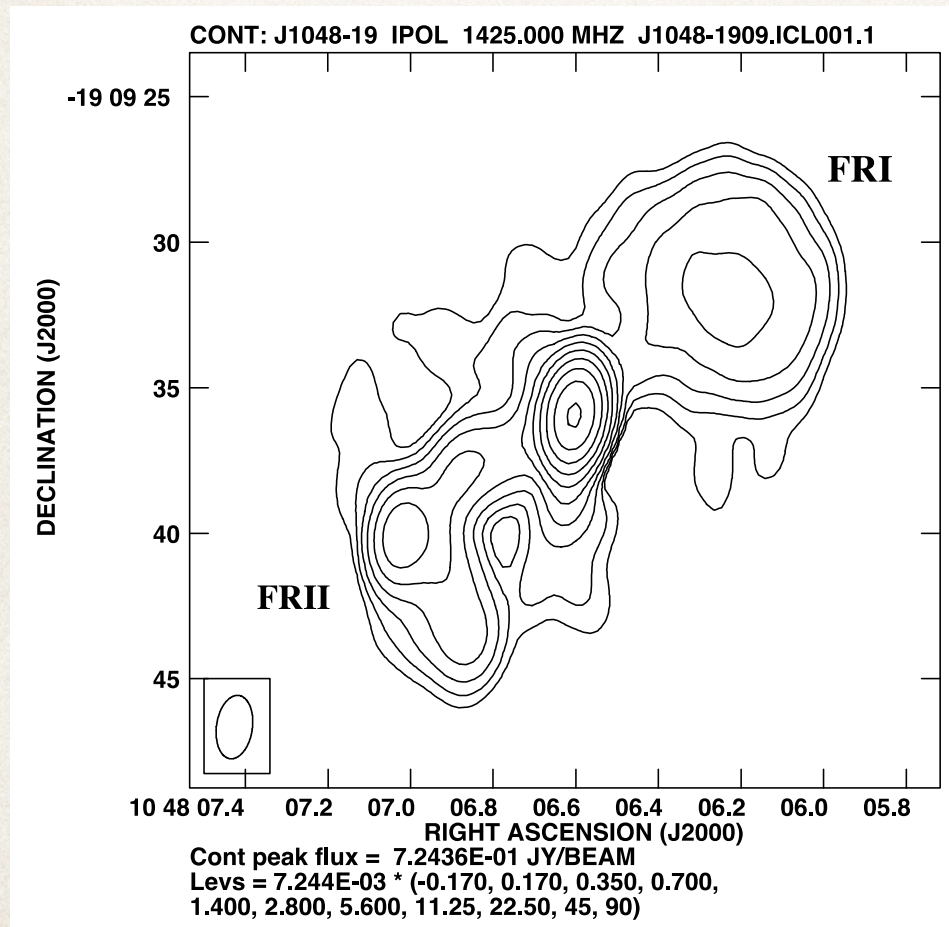


❖ Radio & Optical = Synchrotron

❖ X-ray = IC / CMB

*SED code of Krawczynski 2004
modified to include IC/CMB by
Xue+ 2008*

MOJAVE Hybrid Blazars

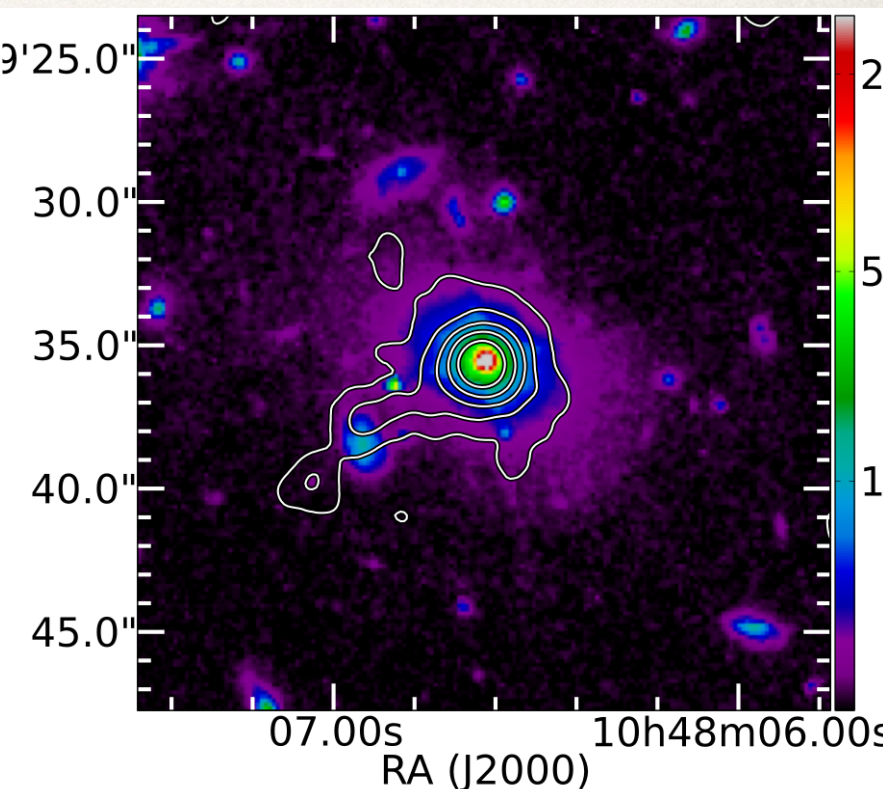
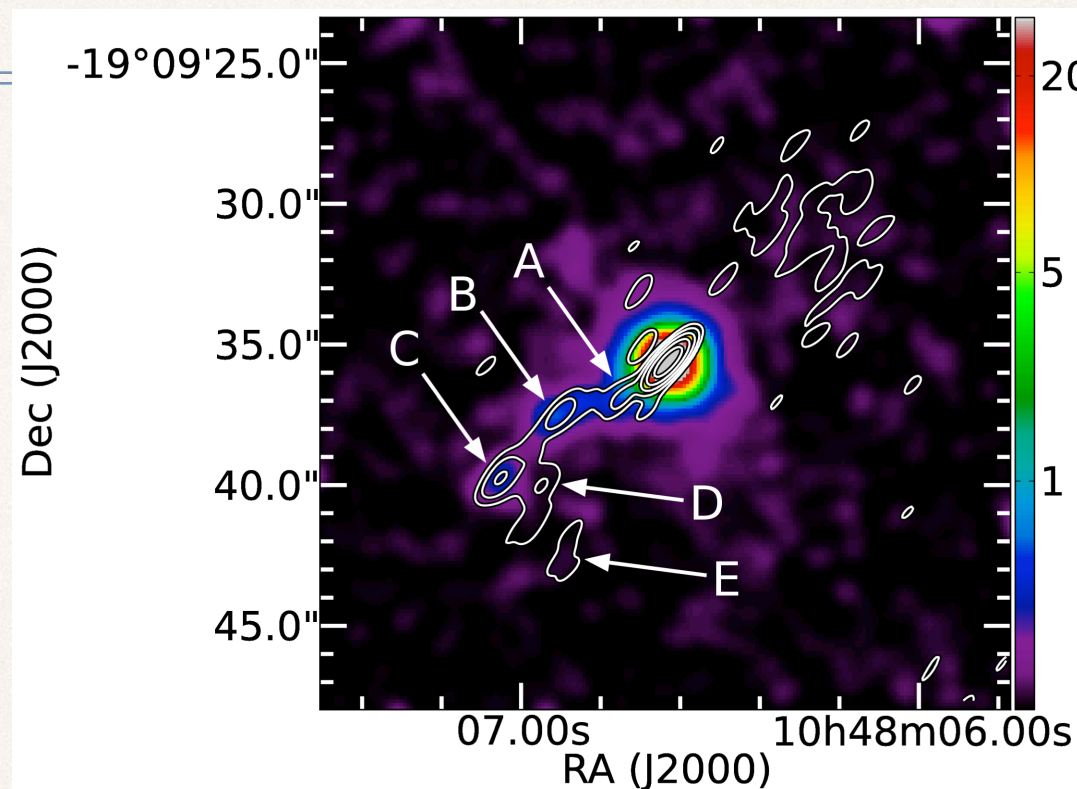


- ❖ Chandra ACIS & HST WFC3/F160W & F475W — MCS blazars 1045-188, 1849+670, 2216-038

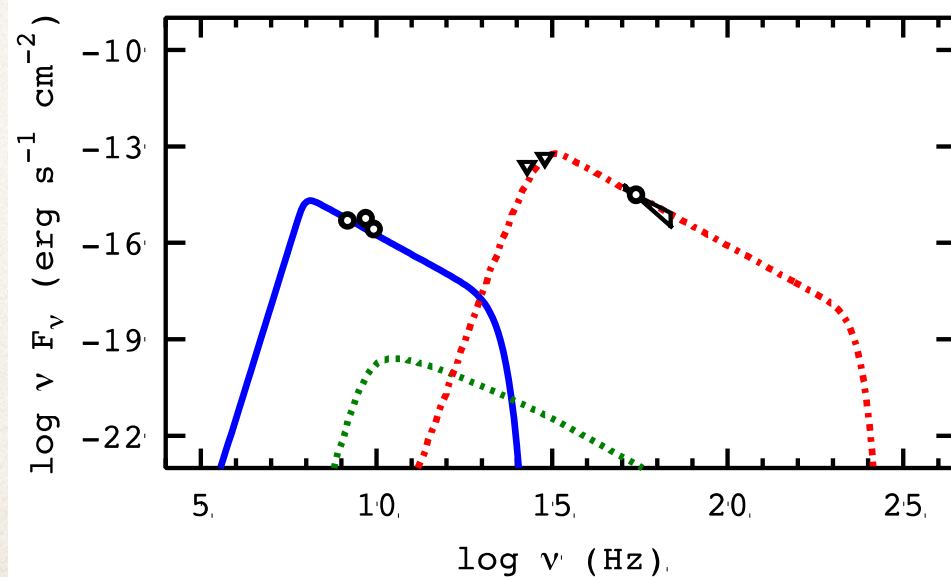
MOJAVE hybrid blazar 1045-188

SED best fits (B, C):

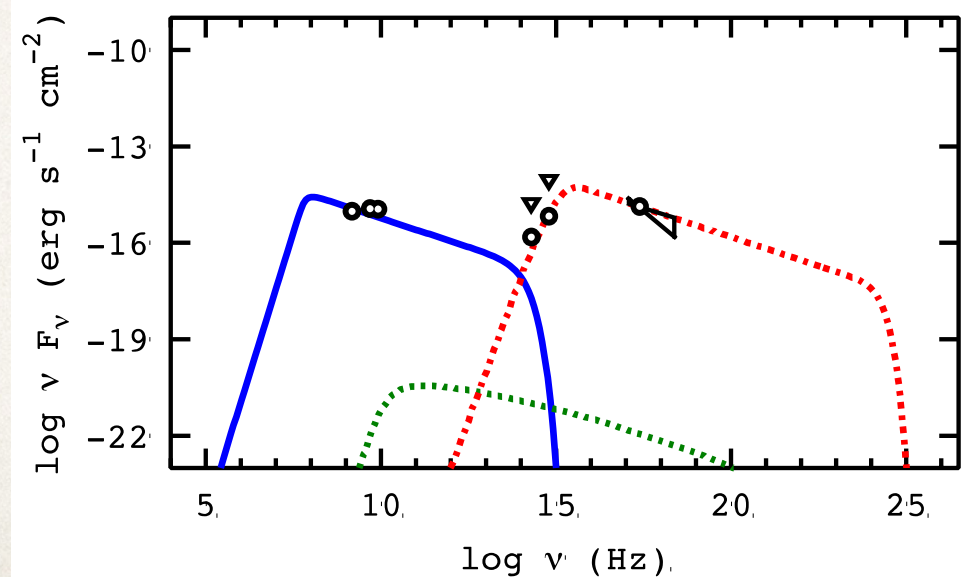
- ❖ $\delta=4.1$
- ❖ $B=50, 60 \mu\text{G}$
- ❖ $\gamma_{\text{min}}=6, 10$
- ❖ $\gamma_{\text{max}}=1-2\text{E}5$
- ❖ $n=4.2, 3.7$



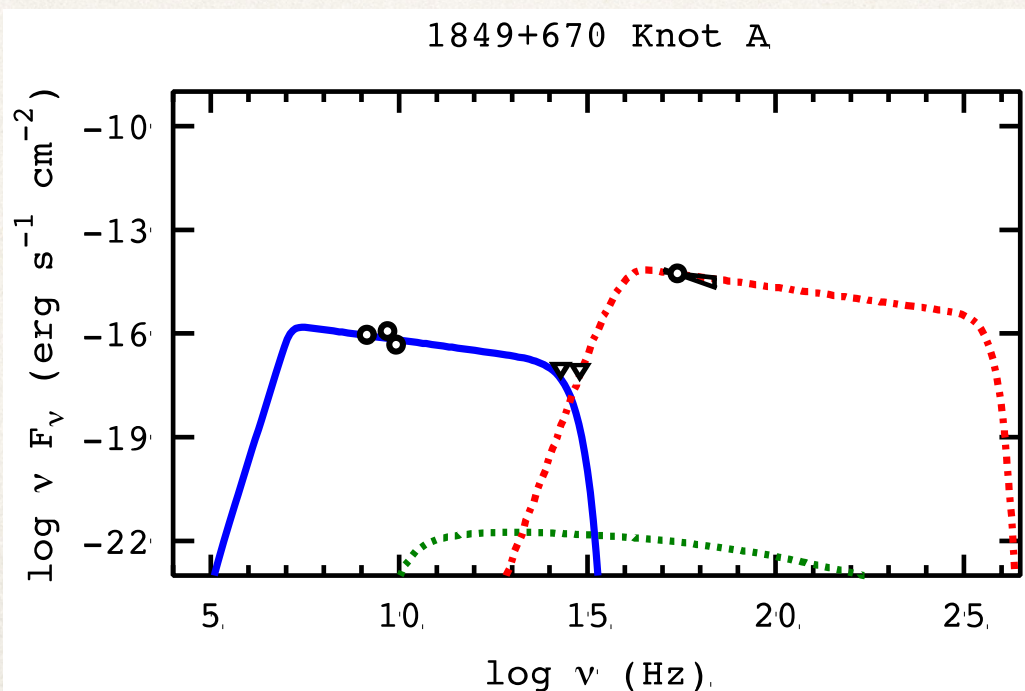
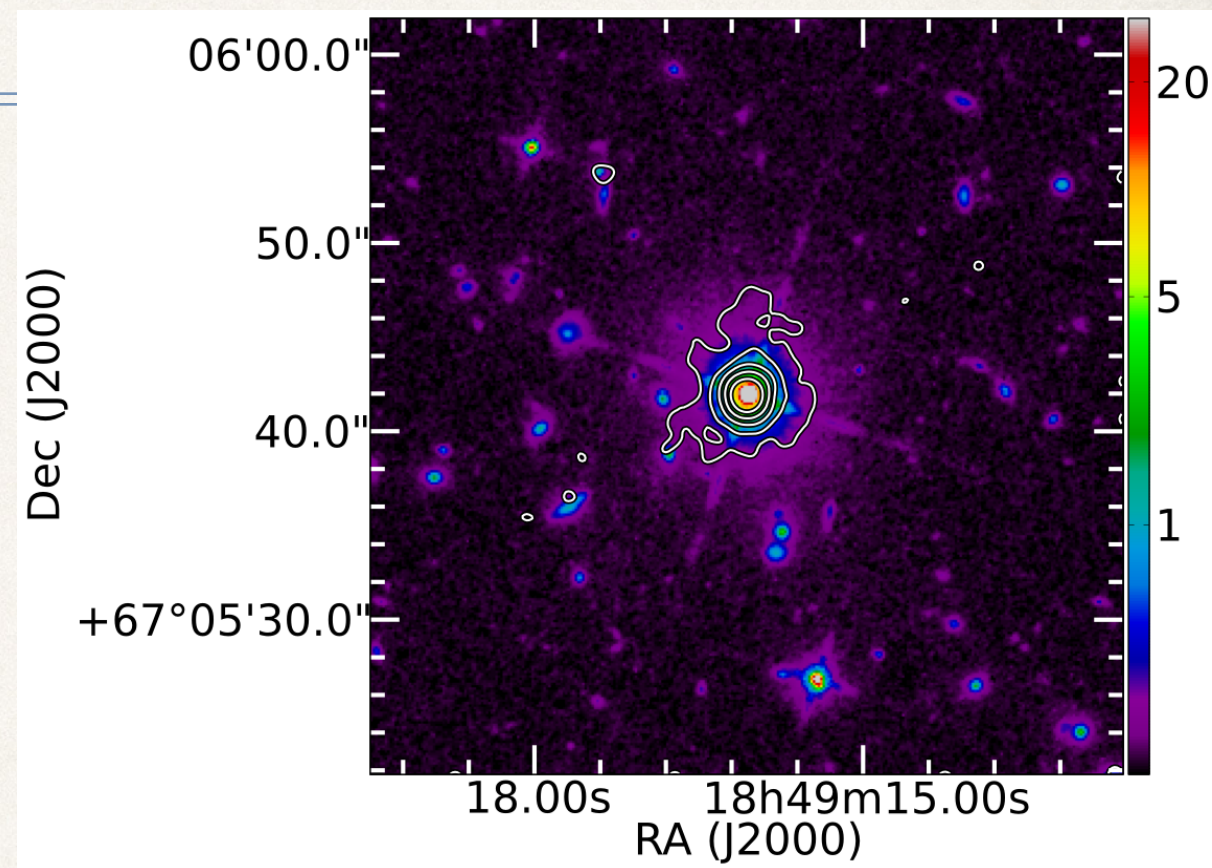
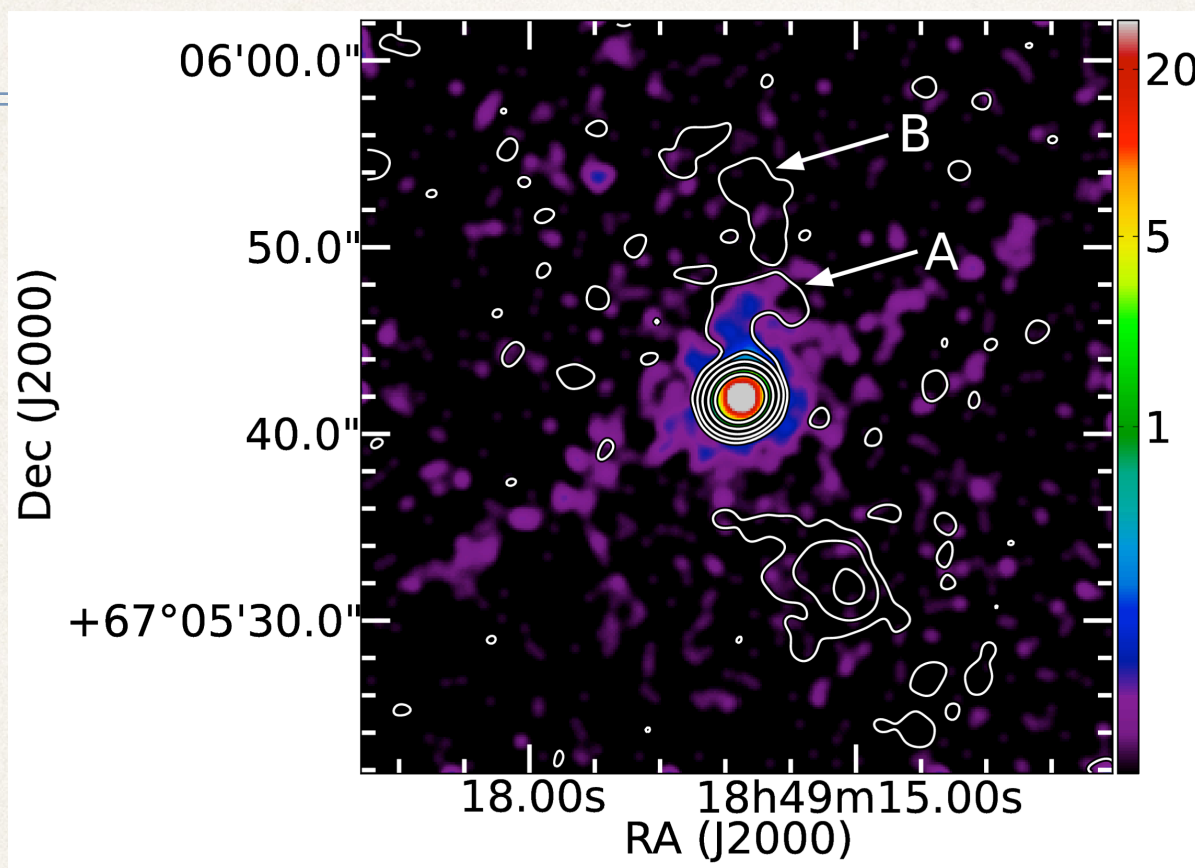
1045-188 Knot B



1045-188 Knot C



MOJAVE hybrid blazar 1849+670



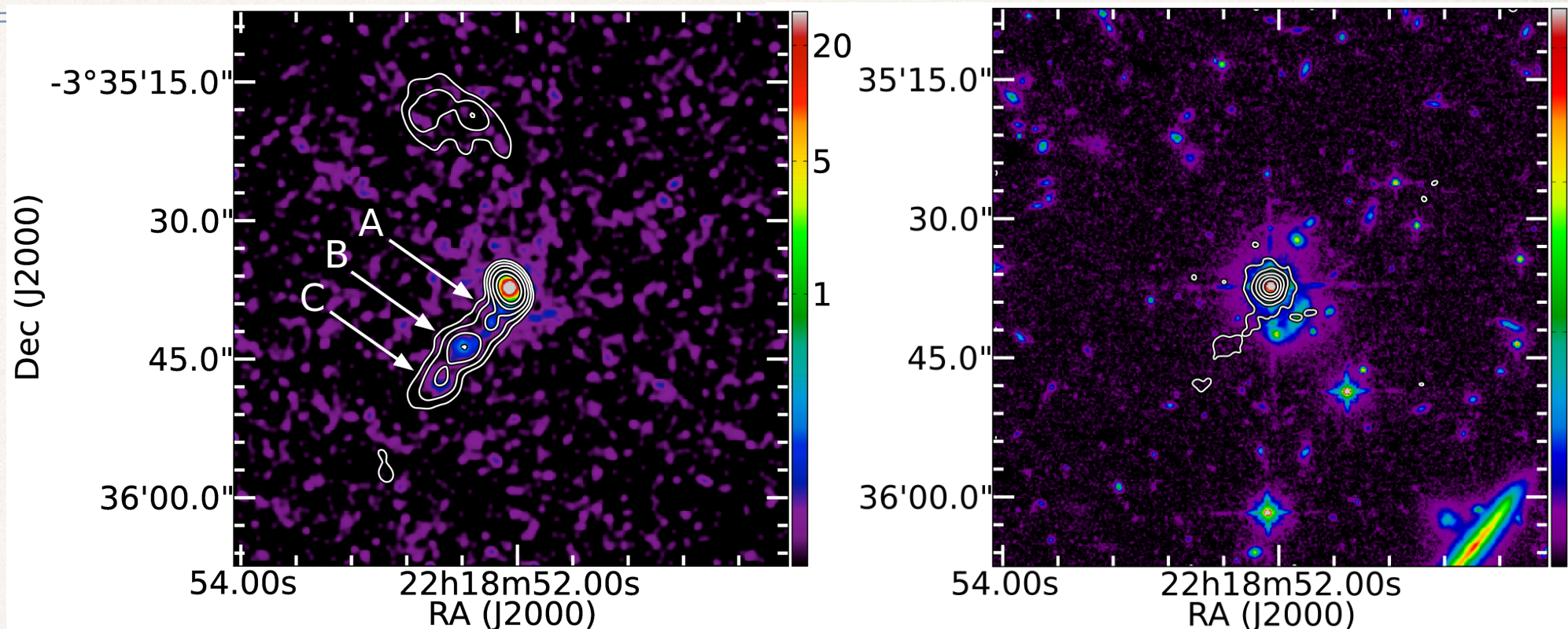
SED best fit (A):

- $\delta=4.2$
- $B=65 \mu\text{G}$
- $\gamma_{\text{min}}=25$
- $\gamma_{\text{max}}=1\text{E}6$
- $n=3.3$

MOJAVE hybrid blazar 2216-038

SED (A, B, C):

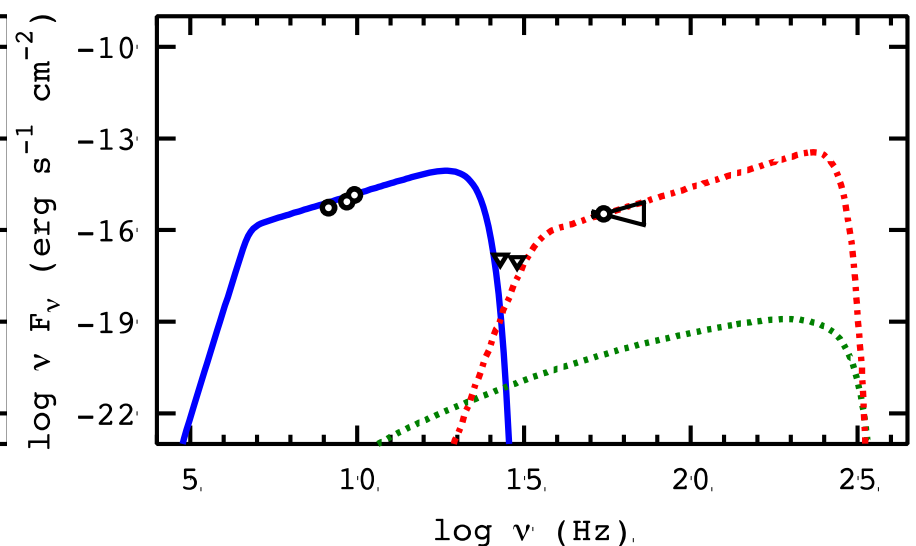
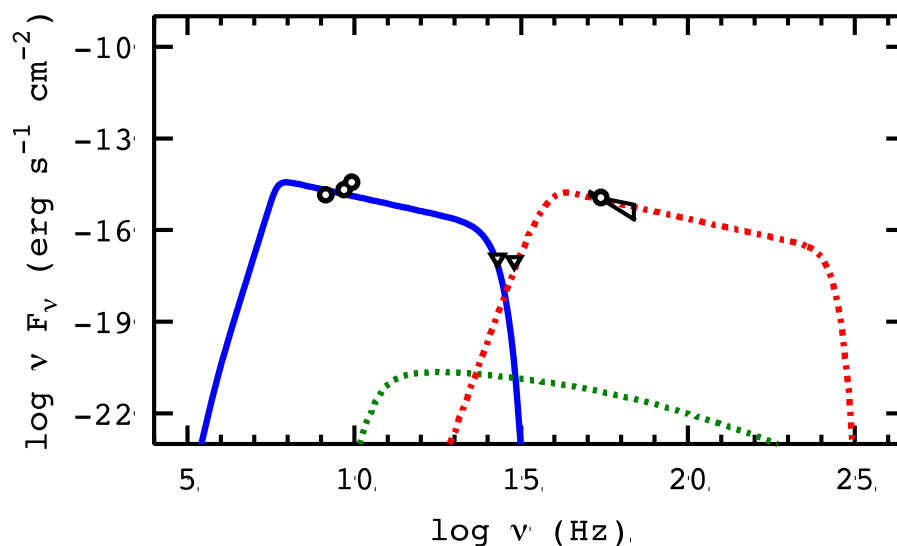
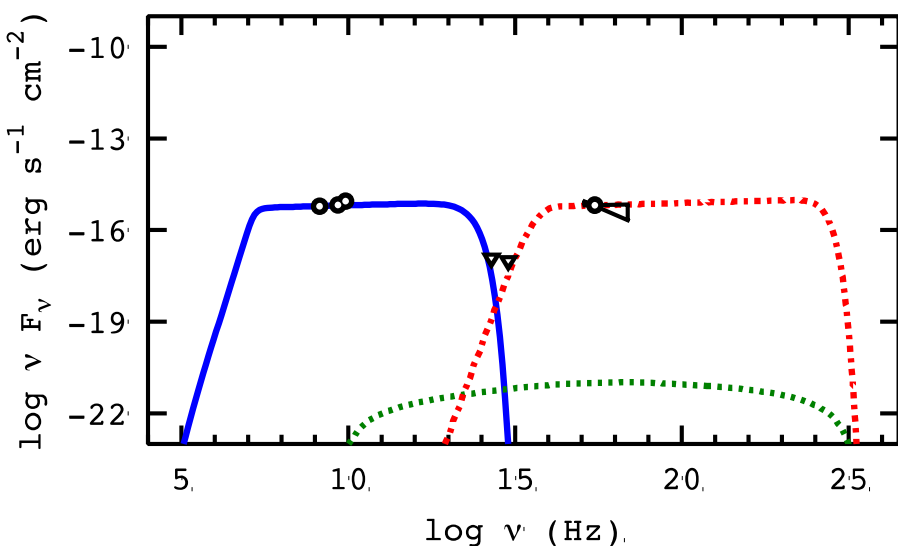
- ❖ $\delta=3.0$
- ❖ $B=25, 70, 15 \mu\text{G}$
- ❖ $\Gamma_{\text{min}}=20, 25, 15$
- ❖ $\Gamma_{\text{max}}=3.1\text{E}5, 2.5\text{E}5, 3\text{E}5$
- ❖ $n=2.9, 3.5, 2.3$



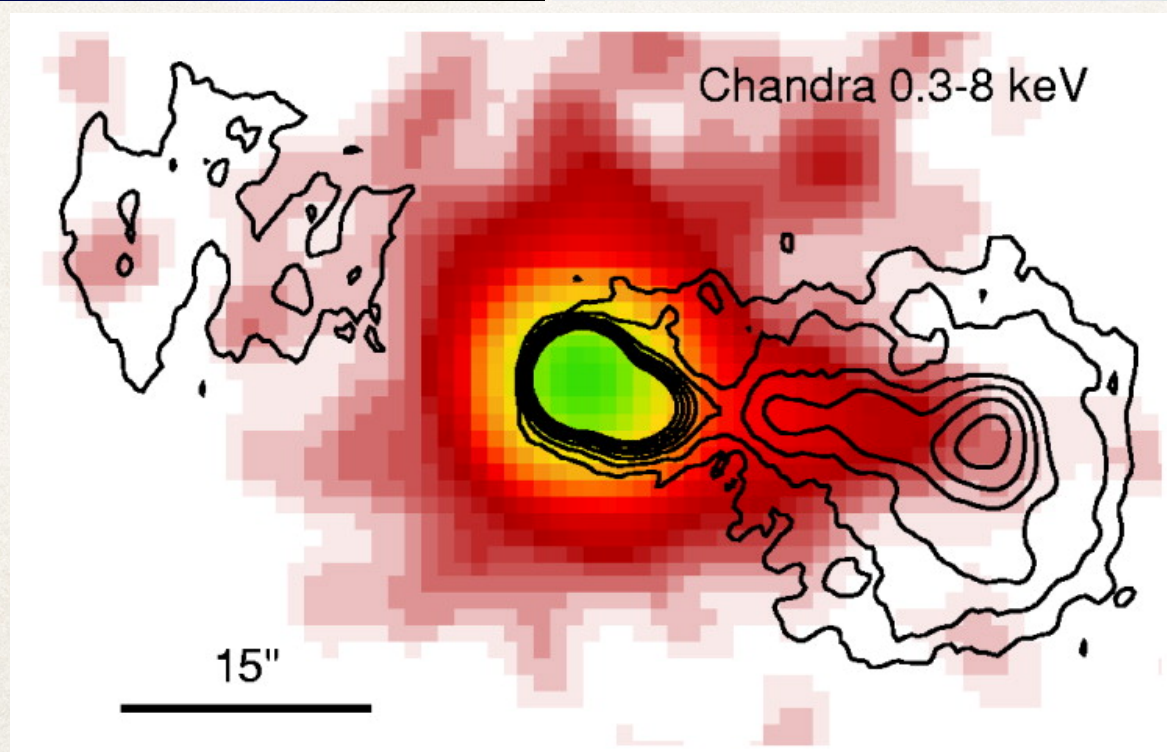
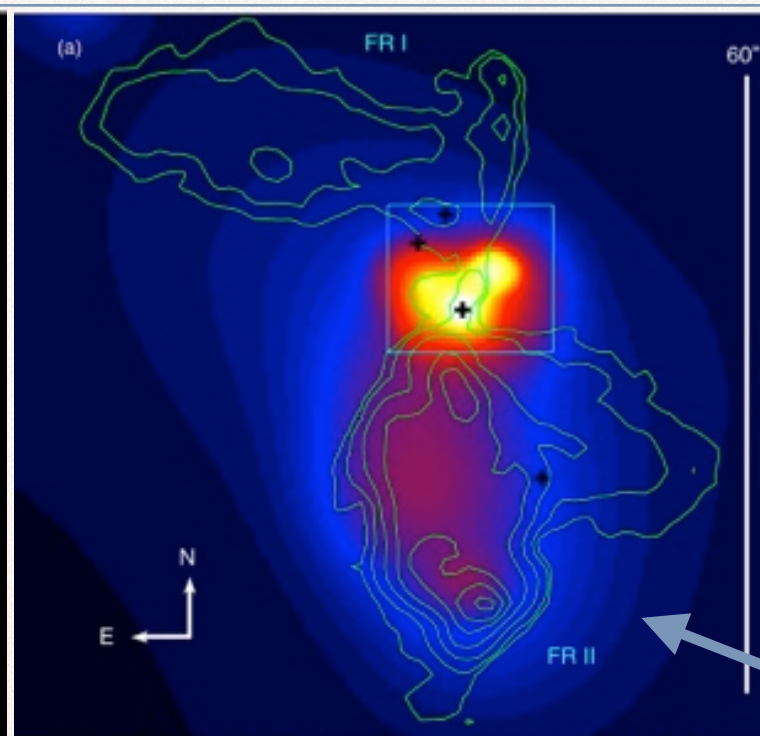
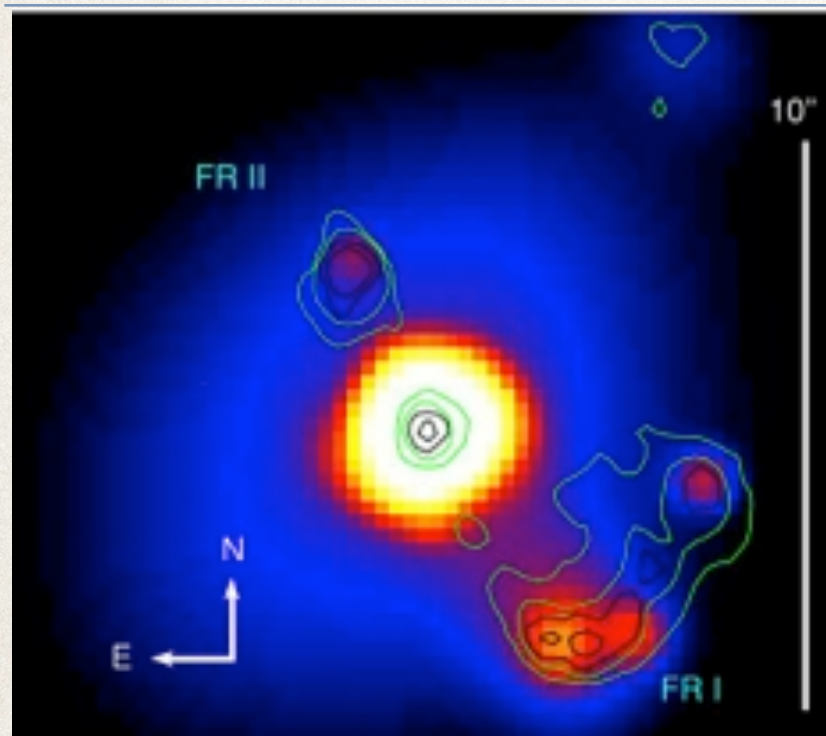
2216-038 Knot A

2216-038 Knot B

2216-038 Knot C



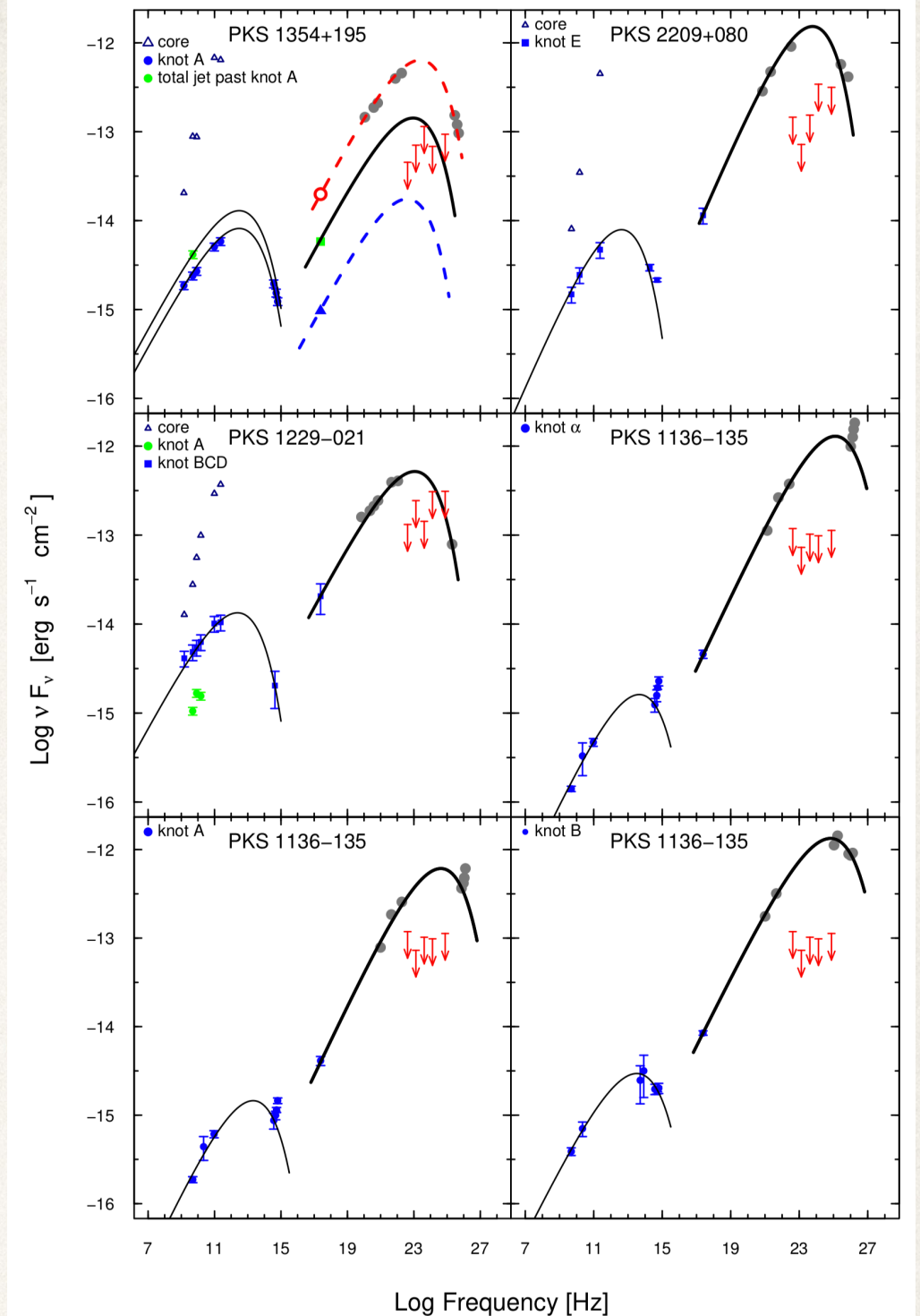
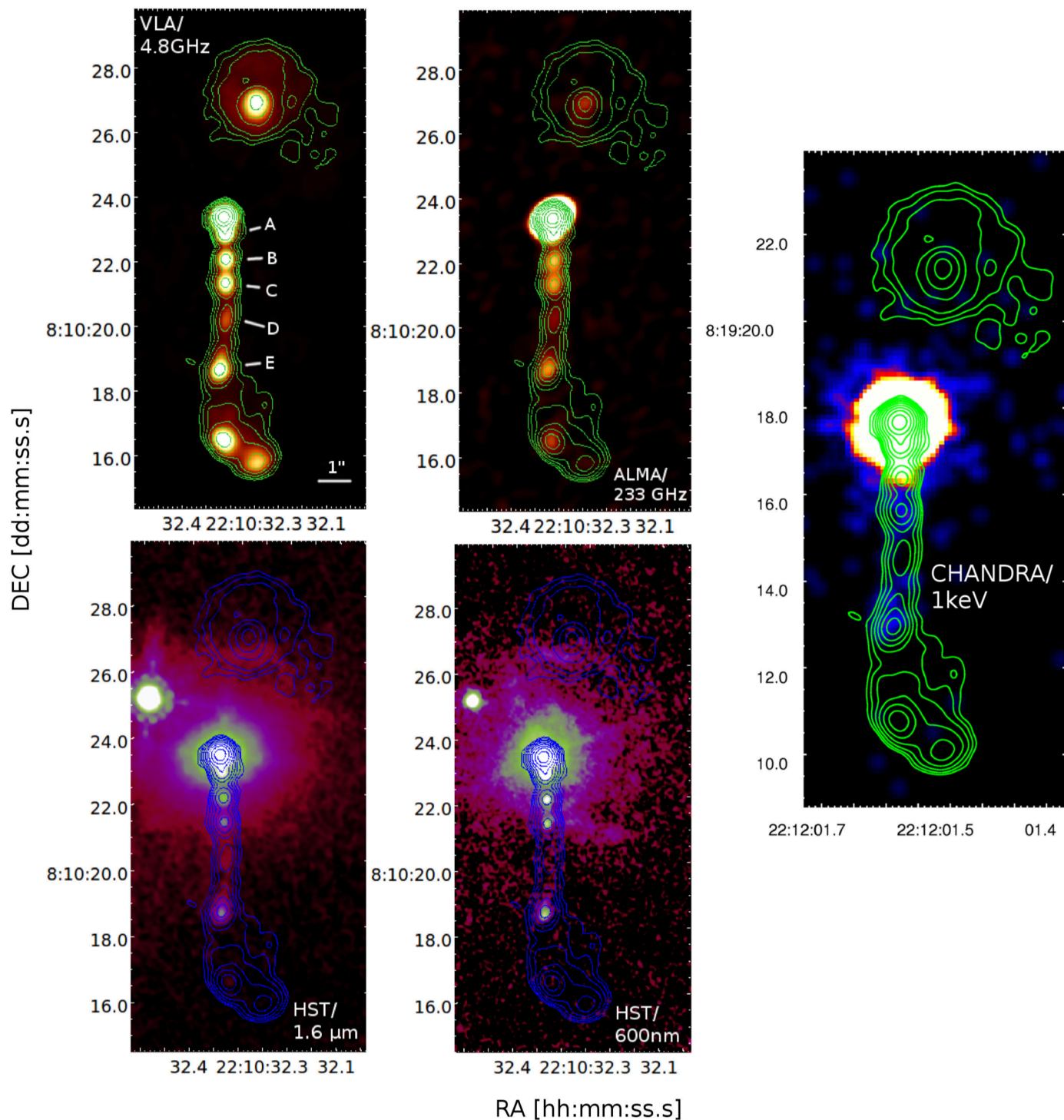
X-rays from Hybrid sources



- ❖ 13 hybrid sources observed with Chandra & HST. IC / CMB in >70% sources

- ❖ X-ray jets IC / CMB (Miller & Brandt, 2009)

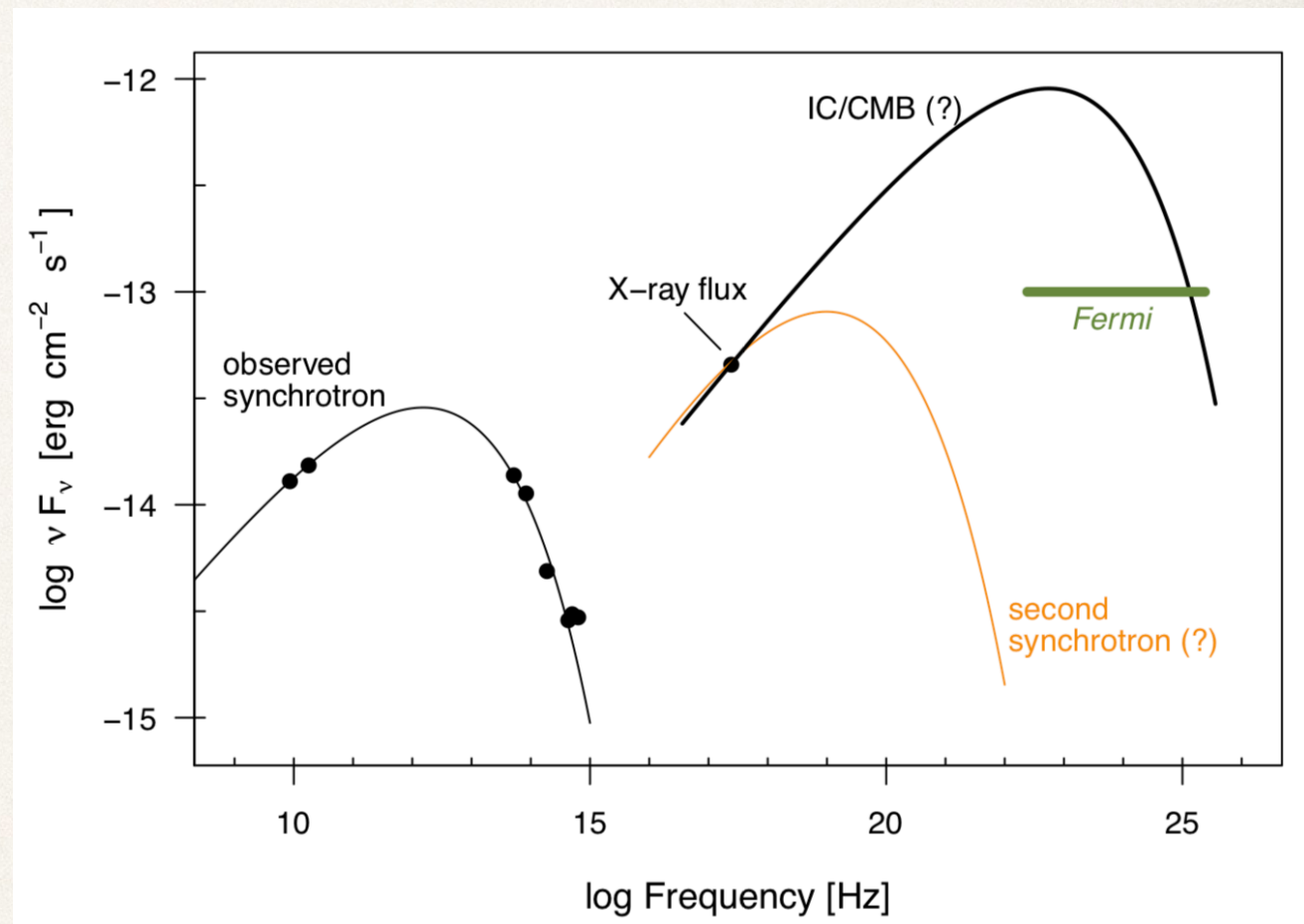
- ❖ X-ray jet Synchrotron (Sambruna+ 2007)



- ❖ Fermi gamma-ray telescope non-detections of many blazar jets challenge IC/CMB. UV in the 2nd hump is highly polarised. X-ray synchrotron ?
- ❖ Second Synchrotron Component in X-rays OR Hadronic Jet Models (Harris+ 2004, Meyer+ 2015, Brieding+ 2017)

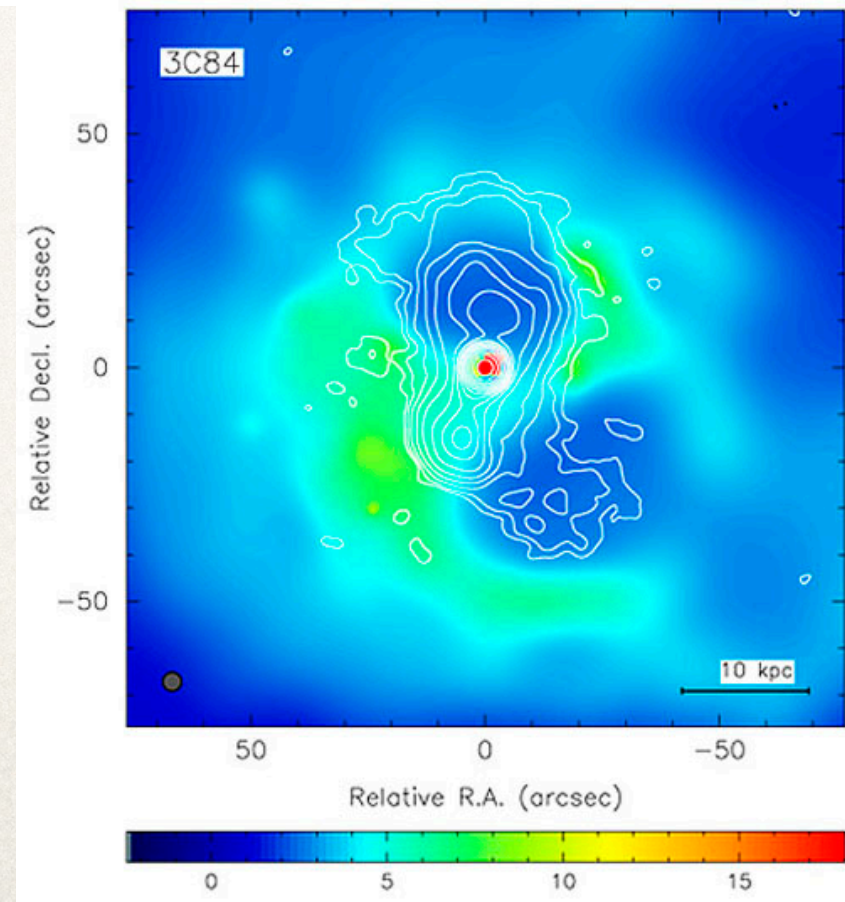
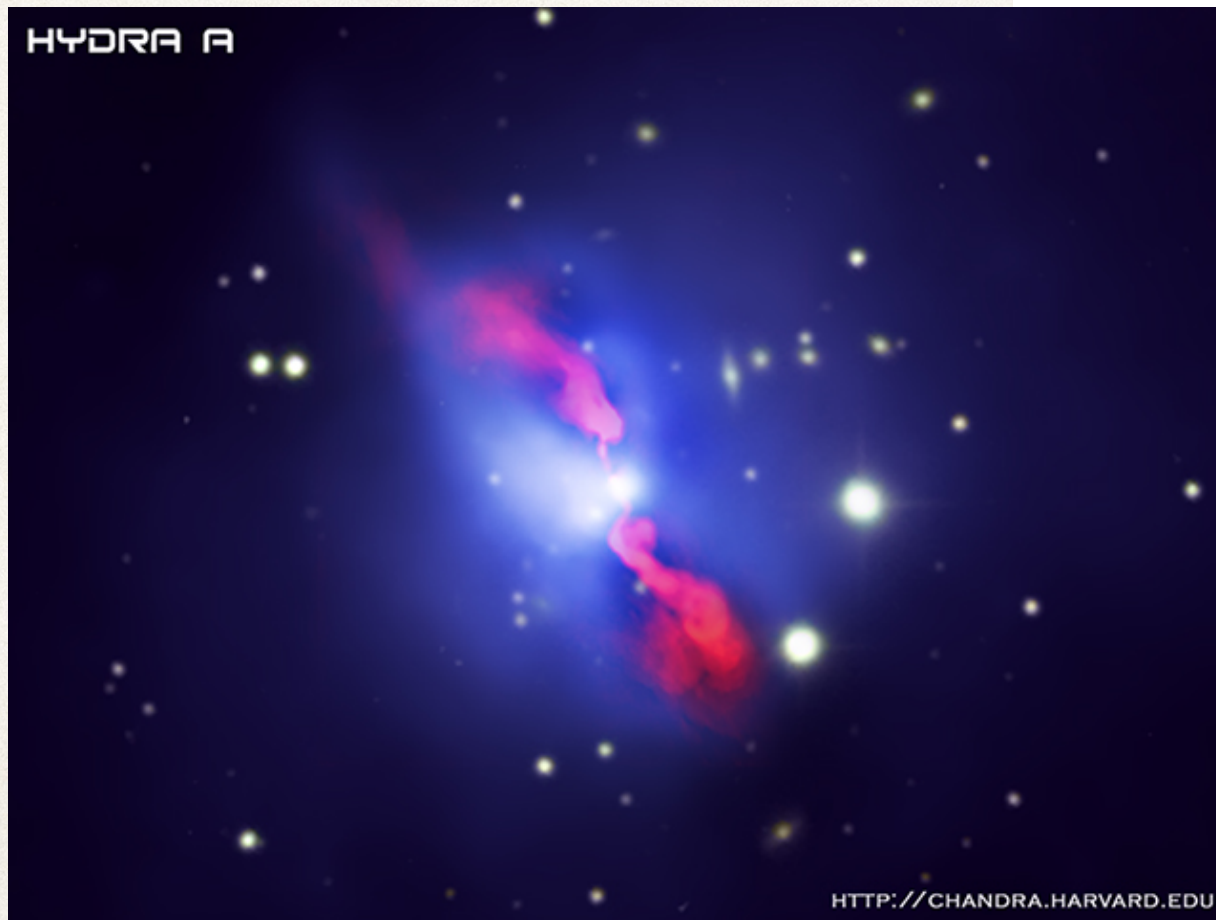
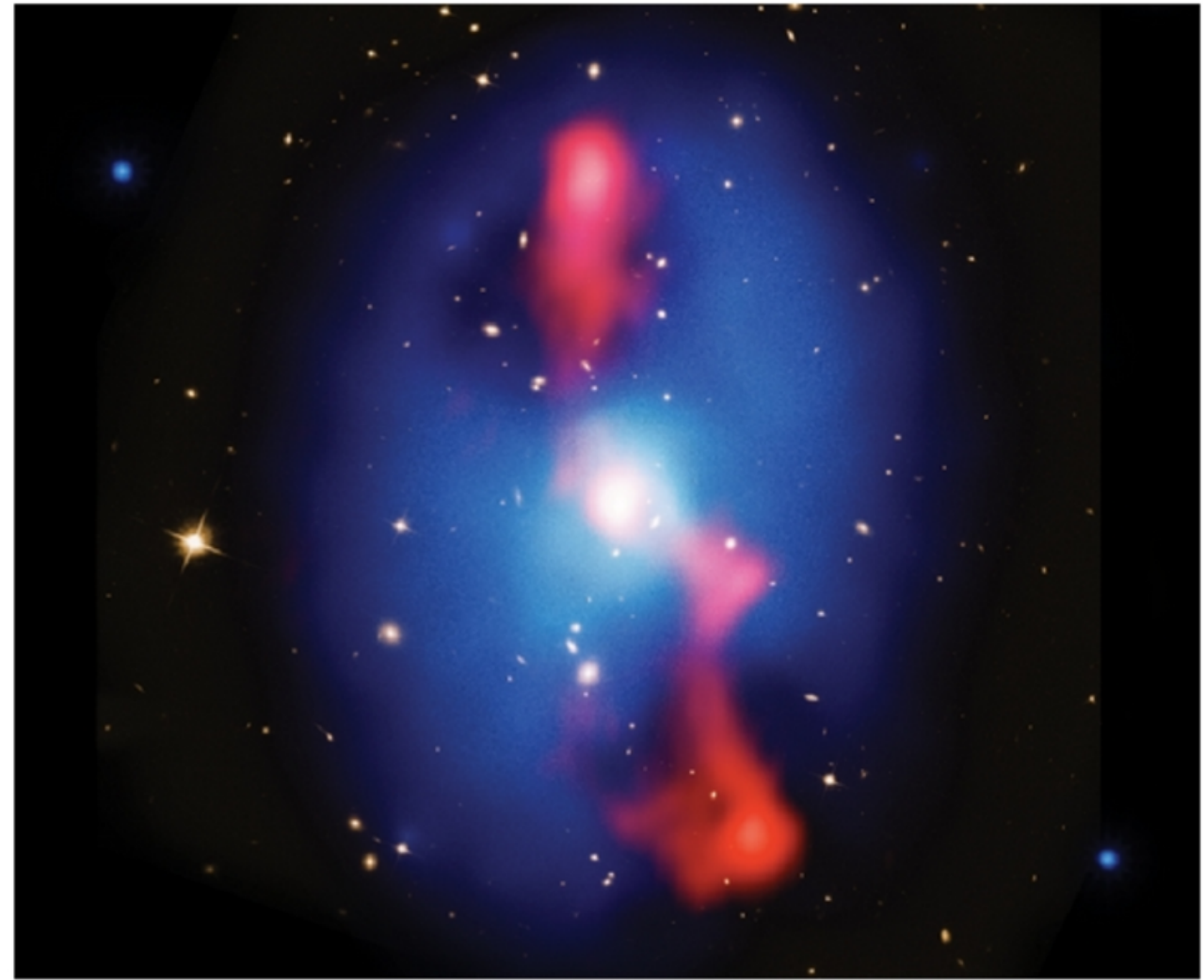
X-ray Emission Mechanisms

- ❖ **Synchrotron:** FRI Jets + some Hybrid Jets
- ❖ **IC/CMB:** FR II Jets + most Hybrid Jets
- ❖ **IC/CMB:** does not work in many blazar jets with Fermi (non-)detections
- ❖ **Second Synchrotron** component in X-rays or **Hadronic Jet Models** (e.g., Meyer+ 2015)
- ❖ *X-rays: Jet Structure, Particle Acceleration & Jet Composition*



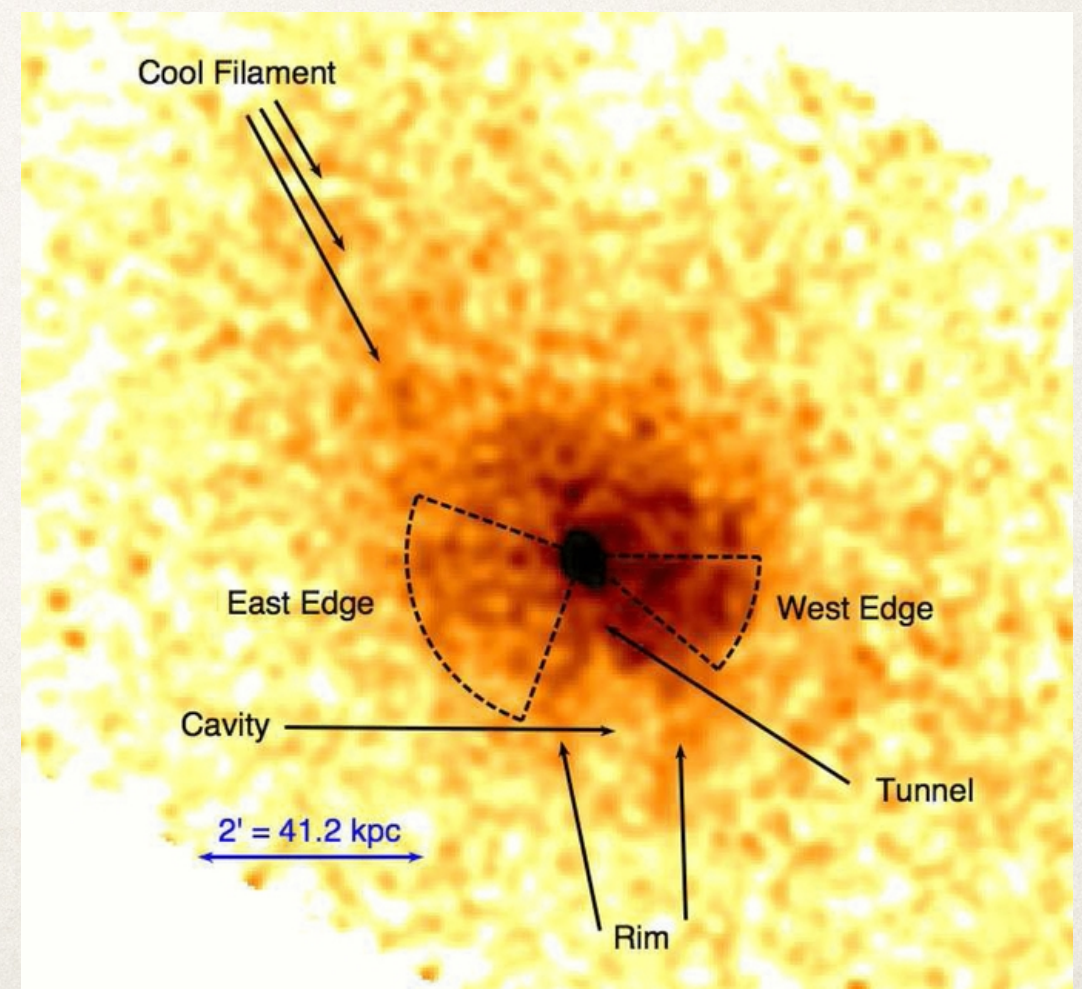
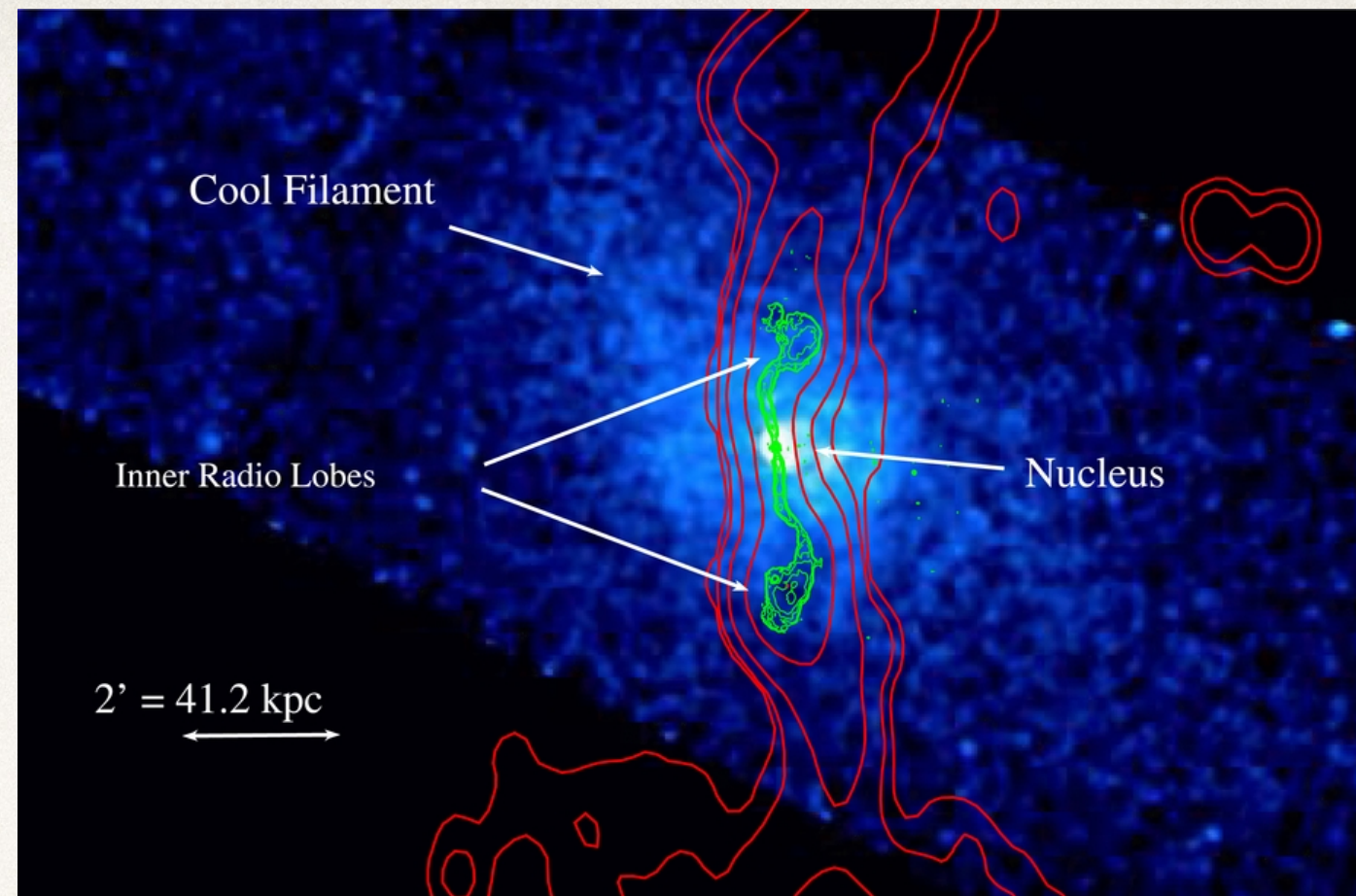
AGN Jets Impact Surrounding Medium

- ❖ Diffuse X-ray emission from Galaxies, Galaxy Groups & Galaxy Clusters — Thermal bremsstrahlung
- ❖ X-ray Cavities
- ❖ AGN Jet feedback offsets “Cooling Flow” in X-rays



Galaxy Merger Histories

- ❖ X-ray emission contains the merger history of the galaxy clusters.
- ❖ 3C449 with Chandra: (1) Cavities & Tunnels (2) Sharp surface brightness Edges — sloshing gas and “cold fronts” from mergers of cool-core galaxy sub-clusters.
- ❖ Lal+ 2013



Summary

- ❖ X-ray Emission — A signature of AGN activity — from Accretion disks & Coronae
- ❖ X-ray Jets are Ubiquitous in Radio-loud AGN
- ❖ Emission mechanisms are not universally established. Vary with Jet type.
- ❖ X-rays inform us about Jet composition + Structure + Acceleration
- ❖ AGN jets impact Galaxy, Galaxy group & cluster environments — X-rays inform us about their internal dynamics & evolution